Uncoupling of the ITIM receptor G6b-B from the tyrosine phosphatases Shp1 and Shp2 disrupts platelet homeostasis in mice

Mitchell J. Geer[1], Johanna P. van Geffen[2], Piraveen Gopalasingam[3], Timo Vögtle[1], Christopher W. Smith[1], Silke Heising[1], Marijke J. E. Kuijpers[2], Bibian M. E. Tullemans[2], Gavin E. Jarvis[4], Johannes A. Eble[5], Mark Jeeves[3], Michael Overduin[3*], Johan W. M. Heemskerk[2], Alexandra Mazharian[1] and Yotis A. Senis[1]

[1]Institute of Cardiovascular Sciences, College of Medical and Dental Sciences, University of Birmingham, Birmingham, United Kingdom
[2]Department of Biochemistry, Cardiovascular Research Institute Maastricht (CARIM), Maastricht University, Maastricht, The Netherlands
[3]Henry Wellcome Building for Biomolecular NMR Spectroscopy, University of Birmingham, Birmingham, UK
[4]Department of Physiology, Development and Neuroscience, University of Cambridge, Cambridge, CB2 3EG, UK
[5]Institute of Physiological Chemistry and Pathobiochemistry, University of Münster, Münster, Germany

Corresponding author:
Yotis Senis, PhD, Professor of Cellular Haemostasis, University of Birmingham, Birmingham, UK, B15 2TT
Email: y.senis@bham.ac.uk
Phone: +44 (0)121 414 8308

[*]Current address: Department of Biochemistry, University of Alberta, Edmonton, Alberta, Canada

Word count:
Abstract: 248
Manuscript: 4,500
Figures/Tables: 7
Supplemental Figures/Tables: 10/2
Supplemental Material: 1,979
References: 26

Running title: Uncoupling of G6b-B-Shp1-Shp2 disrupts platelets

Key words: C6orf25, MPIG6B, G6b-B, megakaryocytes, platelets, thrombocytopenia, hemostasis, transgenic mouse

Key points:

1. Uncoupling of G6b-B from Shp1 and Shp2 results in severe macrothrombocytopenia and aberrant platelet function.

2. G6b-B inhibits CLEC-2 signaling primarily through the protein-tyrosine phosphatase Shp2.

Abstract

The immunoreceptor tyrosine-based inhibitory motif (ITIM)-containing receptor G6b-B has emerged as a key regulator of platelet homeostasis. However, it remains unclear how it mediates its effects. Tyrosine phosphorylation of the ITIM and immunoreceptor tyrosine-based switch motif (ITSM) within the cytoplasmic tail of G6b-B provides a docking site for SH2 domain-containing protein-tyrosine phosphatases Shp1 and Shp2, which are also critical regulators of platelet production and function. In this study, we investigate the physiological consequences of uncoupling G6b-B from Shp1 and Shp2. To address this, we generated a transgenic mouse model expressing a mutant form of G6b-B in which tyrosine (Y) residues 212 and 238 within the ITIM and ITSM were mutated to phenylalanine (F), respectively. Mice homozygous for the mutation (*G6b-B diY/F*) were macrothrombocytopenic, due to a reduction in platelet production, had large clusters of megakaryocytes and myelofibrosis at sites of hematopoiesis, similar to that observed in *G6b* knockout (*G6b KO*) mice. Platelets from *G6b-B diY/F* mice were hypo-responsive to collagen, due to a significant reduction in expression of the immunoreceptor tyrosine-based activation motif (ITAM)-containing collagen receptor complex GPVI-FcR γ-chain, and thrombin, that could be partially rescued by co-stimulating the platelets with ADP. In contrast, platelets from *G6b-B diY/F*, *G6b KO* and megakaryocyte-specific *Shp2 KO* mice were hyper-responsive to antibody-mediated cross-linking of the hemi-ITAM-containing podoplanin receptor CLEC-2, suggesting that G6b-B inhibits CLEC-2-mediated platelet activation through Shp2. Findings from this study demonstrate that G6b-B must engage with Shp1 and Shp2 in order to mediate its regulatory effects on platelet homeostasis.

Introduction

Platelets are small fragments of megakaryocytes (MKs) that play a critical role in thrombosis, hemostasis and maintenance of vascular integrity.[1,2] They do so by adhering to exposed extracellular matrix proteins at sites of vascular injury, where they become activated and form a hemostatic plug, preventing excessive blood loss and stimulating wound repair. The mechanisms required to maintain hemostasis also facilitate the formation of occlusive thrombi, leading to ischemia in acute coronary heart disease and stroke, two of the leading causes of death worldwide. It is therefore critical to understand the molecular mechanisms controlling platelet production and function, in order to devise new and improved ways of regulating these processes.

Immunoreceptor tyrosine-based inhibition motif (ITIM)-containing receptors are important inhibitors of platelet activation.[3] They function through a conserved intracellular ITIM (consensus sequence: I/V/LxYxxL/V),[4] usually in tandem with another ITIM or an immunoreceptor tyrosine-based switch motif (ITSM, consensus sequence: TxYxxV/I).[5] Tyrosine residues within the ITIM and ITSM are phosphorylated by Src family kinases (SFKs), providing docking sites for the structurally-related Src homology 2 (SH2) domain-containing protein-tyrosine phosphatases (PTPs) Shp1 and Shp2.[4] This interaction predominantly inhibits signaling from immunoreceptor tyrosine-based activation motif (ITAM)-containing receptors (consensus sequence: YxxI/Lx_{6-12}YxxI/L). Characterization of knockout (KO) mouse models has also revealed ITIM-containing receptors as regulators of platelet number.[6-8]

G6b-B is a type I transmembrane glycoprotein, consisting of a single extracellular immunoglobulin-like variable-type domain, a transmembrane region and a cytoplasmic tail. The cytoplasmic tail contains a juxtamembrane proline rich region (PRR), an ITIM and a C-terminal ITSM. An inhibitory role for G6b-B in regulating ITAM-mediated platelet activation

was shown using G6b-B-deficient mice (*G6b*$^{-/-}$, referred to as *G6b KO*), and G6b-B-GPVI double-heterozygous mice (*G6b*$^{+/-}$*Gp6*$^{+/-}$).[6] Unexpectedly, *G6b KO* mice also exhibited severe macrothrombocytopenia and aberrant proplatelet formation. Concomitant deletion of GPVI and CLEC-2 failed to fully rescue the *G6b KO* phenotype, suggesting other physiological functions of G6b-B that go beyond inhibiting ITAM receptor signaling.[6] Intriguingly, patients lacking G6b-B exhibit a similar phenotype to that of *G6b KO* mice, including macrothrombocytopenia, megakaryocyte clusters in the bone marrow and myelofibrosis (*Hofmann et al. co-submitted*).[9] Indeed, recent findings using a humanized G6b-B mouse model confirmed that human and mouse G6b-B perform analogous physiological functions (*Hofmann et al. co-submitted*).

G6b-B is thought to mediate its functions through association with Shp1 and Shp2.[6,10] Activation of Shp phosphatases depends upon phosphopeptide binding of the N-terminal SH2 domain, which normally blocks access of substrates to the PTP catalytic site.[11] MK-specific Shp2, and to a lesser extent Shp1, KO mouse models (*Ptpn11*$^{fl/fl}$*;PF4-Cre*$^{+}$ and *Ptpn6*$^{fl/fl}$*;Pf4-Cre*$^{+}$, referred to as *Shp2 KO* and *Shp1 KO*, respectively), phenocopy multiple features of *G6b KO* mice.[12] However, Shp1/Shp2 conditional double-KO mice (*Ptpn6*$^{fl/fl}$*;Ptpn11*$^{fl/fl}$*;Pf4-Cre*$^{+}$, referred to as *Shp1/Shp2 DKO*) exhibited a more severe phenotype than *G6b KO* mice,[12,13] demonstrating additional roles of Shp1 and Shp2 in MKs and platelets.

The aim of this study was to determine the role of G6b-B-mediated compartmentalization of Shp1 and Shp2 in regulating platelet production and function. To address this, we generated and characterized a novel knock-in (KI) mouse model, in which tyrosine (Y) residues 212 and 238, within the ITIM and ITSM of G6b-B were mutated to phenylalanine (F), respectively. Mice homozygous for these *loss-of-function* mutations (*G6b*$^{diYF/diYF}$, referred to as *G6b-B diY/F*) were severely macrothrombocytopenic and

showed a significant downregulation of the ITAM-containing GPVI-FcR γ-chain complex, highlighting the critical role of Shp1 and Shp2 recruitment to G6b-B for it to mediate its biological effects. We also demonstrate that the inhibitory effect of G6b-B on CLEC-2 signaling is primarily mediated by Shp2, as well as providing structural insights into the interaction between phosphorylated G6b-B and Shp2.

Materials and methods

Antibodies and reagents

FITC-conjugated P-selectin, GPVI, GPIbα and α2, and R-phycoerythrin (PE)-conjugated JON/A antibodies were from Emfret Analytics (Eibelstadt, Germany); PE-conjugated anti-αIIb antibody from BD Biosciences (Oxford, UK); fibrinogen-488 and phalloidin-488 from Thermo Fisher (Loughborough, UK); rat anti-mouse CLEC-2 antibody and IgG_{2B} isotype control antibody from Serotec (Oxford, UK) and Alexa488-conjugated goat anti-rat antibody from Life Technologies (Paisley, UK). G6b-B specific antibodies were raised as previously described.[6] For immunoblotting, anti-Shp1 and anti-Shp2 antibodies were from Santa Cruz Biotechnology (Dallas, TX, USA); anti-phosphotyrosine (p-Tyr); FcR γ-chain and PAR4 antibodies from Merck Millipore (Nottingham, UK); Src phosphotyrosine-418 (Src p-Tyr418) from Life Technologies (Loughborough, UK) and Syk phosphotyrosine-525/26 (Syk p-Tyr525/526) from Cell Signaling Technology (Hitchin, UK). All other reagents were from Sigma-Aldrich (Poole, UK).

Mice

The *G6b-B diY/F KI* mouse model was generated as outlined in the supplementary methods (Taconic Biosciences, Cologne, Germany). *G6b* constitutive *KO* and conditional *Shp1* and *Shp2 KO* mouse models, referred to as *G6b KO, Shp1 KO* and *Shp2 KO*, respectively, were generated as previously described. [6,12] Genotypes of litter matched control mice (*WT*) were $G6b^{+/+}$, $Ptpn6^{fl/fl}$;*Pf4-Cre*$^{-}$ and $Ptpn11^{fl/fl}$;*Pf4-Cre*$^{-}$. All mouse models used in this study were on a C57BL/6 background. Procedures were undertaken with UK Home Office approval, in accordance with the Animals (Scientific Procedures) Act of 1986.

Statistical analysis

All data is presented as mean ± standard error of the mean (SEM), unless stated otherwise. Statistical significance was analyzed either by Student's *t*-test or two-way ANOVA, followed by the indicated *post hoc* test, using GraphPad Prism 6 (GraphPad Software, Inc., La Jolla, CA), unless stated otherwise.

Detailed descriptions of all other methods can be found in Supplementary Methods.

Results

Verification of *G6b-B diY/F* mouse model

To determine the physiological importance of the interaction between G6b-B-Shp1-Shp2 in platelet production and function, we generated a *G6b-B diY/F* mouse model (Figure S1) expressing a mutant form of G6b-B that is unable to engage with Shp1 or Shp2. The specific abolition of Shp1 and Shp2 docking sites allowed for delineation of the importance of this binding event and downstream signaling, independent of other potential signaling events. *G6b-B diY/F* mice were born at Mendelian frequencies (Table S1), were fertile and survived >25 weeks without any overt developmental or growth defects. Both surface and total protein expression of G6b-B diY/F in platelets from *KI* mice was comparable to that of G6b-B in platelets from *WT* mice (Figure 1A, B). As expected, neither Shp1 nor Shp2 co-immunoprecipitated with G6b-B diY/F from resting or collagen-stimulated platelets (Figure 1C), demonstrating that interactions between G6b-B-Shp1-Shp2 were indeed lost. Immunoprecipitation of Shp2 also confirmed absence of the interaction (Figure S2).

Reduced platelet production in *G6b-B diY/F* mice

G6b-B diY/F mice were severely macrothrombocytopenic, as observed in *G6b KO* mice. Platelet count was reduced by 76% and platelet volume increased by 36% in *G6b-B diY/F* mice, compared with *WT* mice (Table S2). These changes were independent of age (Figure S3). Increased platelet volume is frequently associated with immature platelets, which was confirmed by an increased proportion of reticulated platelets in *G6b-B diY/F* mice (Figure 2A). Thrombocytopenia in these mice was not a consequence of reduced platelet lifespan, measured as the proportional slope to give the rate of clearance of biotinylated platelets from the circulation (Figure 2B).

As clearance was normal, reduced platelet counts had to be due to defects in production. We therefore investigated platelet recovery following anti-GPIbα antibody-

mediated depletion (Figure 2Ci). Proportional slopes for days 3-7 were calculated and compared for *WT* and *G6b-B diY/F* mice. A four-fold reduction in the number of platelets produced per day was identified in *G6b-B diY/F* mice compared with *WT* mice (Figure 2Cii), suggesting aberrant platelet production by MKs. This was supported by increased MK clusters and myelofibrosis in spleens and femurs, and an 86% increase in spleen:body weight ratio (Figure 2D). MKs tended to be localized in distinct large clusters throughout the bone marrow and red pulp of spleens, similar to that observed in G6b-B-deficient patients (*Hofmann et al, co-submitted*). Interestingly, lymphocyte counts were also increased in *G6b-B diY/F* mice, as observed in both patients and *G6b KO* mice, likely due to inflammation caused by the severe myelofibrosis.

Increased bleeding is caused by aberrant platelet function in *G6b-B diY/F* mice

A primary function of platelets is to prevent blood loss following injury. We therefore investigated the effect of loss of G6b-B-Shp1-Shp2 interactions on hemostasis. Overall, blood loss increased in both *G6b-B diY/F* and *G6b KO* mice, although for both genotypes there were mice with apparently normal bleeding (Figure 3A). The probability of abnormal bleeding in GM mice was determined by modelling blood loss to a bimodal distribution. The probability of abnormal bleeding in *G6b-B diY/F* mice was 0.47 [0.23, 0.72] (mean [95% CI]) and for *G6b KO* mice was 0.79 [0.49, 0.94]. Pairwise testing between the 3 groups (likelihood ratio test with no adjustment for multiple testing) indicated a clear difference between *WT* (probability of increased bleeding = 0) and both *G6b-B diY/F* (P = 0.0006) and *G6b KO* (P = 1.0 x 10^{-6}) mice. Although *G6b-B diY/F* mice had a lower probability of bleeding than *G6b KO* mice, the difference was less clear-cut (P = 0.071). Since platelet counts must drop by more than 90% for defective hemostasis to be observed,[14] aberrant platelet function is the most likely underlying explanation of this bleeding phenotype, warranting further investigation.

To determine the cause of platelet functional defects, we measured surface receptor expression levels in *G6b-B diY/F* mice by flow cytometry (Figure S4). Expression of GPVI, the main receptor facilitating signaling in response to collagen, was reduced by 81%. Only minor changes were observed in other platelet receptors: 22% reduction in the collagen integrin α2 subunit, 7% increase in the fibrinogen integrin αIIb subunit and 20% reduction in CLEC-2 expression. GPIbα surface expression was unaltered. Western blotting showed comparable expression levels of the receptors investigated by flow cytometry, and a small increase in the thrombin receptor PAR4 (Figure S5). Interestingly, alterations in receptor levels did not fully correlate between *G6b-B diY/F* and *G6b KO* mice, GPIbα levels were significantly reduced in *G6b KO* platelets,[6] suggesting residual functional roles of *G6b-B diY/F*. This may explain differences in bleeding distributions in *G6b-B diY/F* and *G6b KO* mice, described above.

We next set out to identify how these changes in receptor expression affect platelet function. Due to the severe thrombocytopenia of *G6b-B diY/F* mice, a flow cytometry-based assay was first used to assess platelet activation in whole blood. P-selectin exposure and fibrinogen-binding were used as markers of α-granule release and αIIbβ3 integrin activation, respectively. Not surprisingly, responses to the GPVI-specific agonist collagen-related peptide (CRP) were significantly reduced in *G6b-B diY/F* platelets (Figure 3B). Neither was a consequence of reduced P-selectin or αIIbβ3 expression (Figure S4, 5). Convulxin, a more potent GPVI agonist than CRP, induced higher levels of P-selectin exposure and fibrinogen-binding in *G6b-B diY/F* platelets, but still failed to reach levels observed in *WT* platelets (Figure 3B). P-selectin exposure was marginally reduced in *G6b-B diY/F* platelets in response to antibody-mediated cross-linking of CLEC-2, whereas fibrinogen-binding was normal (Figure 3B).

No difference was observed between *G6b-B diY/F* and *WT* mice in response to ADP or the TxA_2 analogue U46619, both of which elicited only weak responses when used either alone or in combination (Figure 3C). However, P-selectin surface exposure was significantly reduced in *G6b-B diY/F* platelets in response to thrombin and PAR4 peptide (Figure 3Ci). Fibrinogen-binding was normal in response to thrombin and reduced in response to PAR4 peptide (Figure 3Cii), presumably because thrombin also binds to GPIbα and is a more potent agonist than PAR4 peptide. Interestingly, P-selectin surface exposure was not rescued in *G6b-B diY/F* platelets co-stimulated with 10 μM ADP and PAR4 peptide (Figure 3Di). In contrast, αIIbβ3 activation was increased to levels observed in *WT* mouse platelets (Figure 3Dii), suggesting a more severe impairment in α-granule release than integrin activation. Comparable results were obtained for most agonists using washed platelets at a normalized count (2×10^7/mL) (Figure S6). Interestingly *G6b-B diY/F* platelets showed increased CLEC-2 antibody-mediated P-selectin exposure and unaltered PAR4 peptide-stimulated fibrinogen binding compared to *WT*, both of which were significantly reduced in whole blood activations. Increased relative levels of secondary activators, such as ADP and TxA_2, which are known to be essential for CLEC-2 signaling,[15] and contributed to the PAR4-mediated defect (Figure 3D), are likely responsible for these differences. Albeit an effect of the platelet washing procedure cannot be excluded.

To further investigate platelet functional defects, we measured platelet aggregation and ATP secretion from dense granules, in response to select agonists by lumi-aggregometry. Moderate reductions in aggregation and ATP secretion were observed in *G6b-B diY/F* compared with *WT* platelets in response to 30 μg/mL collagen, whilst platelets from *G6b-B diY/F* mice failed to respond to 30 μg/mL CRP (Figure 4A, S7). In contrast, *G6b-B diY/F* platelets, which exhibited a minor reduction in CLEC-2 expression, responded more rapidly to 3 μg/mL anti-CLEC-2 antibody than *WT* platelets (Figure 4A, S7). No

difference was seen when platelets were stimulated with 3 nM of the tetravalent, CLEC-2 binding snake toxin rhodocytin (Figure 4A and S5), which is a more robust agonist than the divalent anti-CLEC-2 antibody. The amplitude of platelet aggregation was marginally reduced in *G6b-B diY/F* platelets in response to 0.06 U/mL thrombin and 10 μM U46619, correlating with decreased ATP secretion (Figure 4A, S7). Aggregation was also significantly reduced in response to 10 μM ADP (Figure 4A, S7). Taken together, these findings demonstrate moderate to severe impairments in platelet aggregation and ATP secretion to all agonists tested, except for anti-CLEC-2 antibody, which was enhanced.

Integrin αIIbβ3 activation and outside-in signaling were next interrogated by analyzing platelet adhesion and spreading on fibrinogen (Figure 4B). The number of adhered platelets, platelet perimeter and surface area coverage of *G6b-B diY/F* platelets were normal compared with *WT* platelets, under basal conditions. However, *G6b-B diY/F* platelets failed to maximally spread following pre-activation with 0.1 U/mL thrombin (Figure 4Bi, ii), correlating with the reduced P-selectin exposure to thrombin described above (Figure 3Bi). Morphological analysis of thrombin treated platelets revealed a significant increase in *G6b-B diY/F* platelets with filopodia and concomitant decrease in those forming lamellipodia, compared with *WT* platelets (Figure 4Bv), likely due to defective thrombin-mediated platelet activation identified in aggregation studies.

In light of these defects in platelet activation and function in response to specific agonists, a more physiologically relevant flow adhesion-based assay was performed to assess platelet recruitment to three surfaces: collagen; von Willebrand Factor binding peptide (vWF-BP) and laminin; and vWF-BP, laminin and rhodocytin (Figure 5). Platelet adhesion to vWF-BP-laminin, via GPIbα and the integrin α6β1, respectively, are important for initial platelet rolling and adhesion to exposed extracellular matrix. A shear rate of 1,000s^{-1} was chosen as a standard for phenotyping mice, to allow investigation of both

hemostasis and thrombosis. Under almost all conditions tested *G6b-B diY/F* and *G6b KO* platelet adherence and thrombus formation were significantly reduced when quantifying morphological parameters and surface area coverage (Figure 5A, C). Thrombus contraction and multilayer thrombus formation were also significantly reduced upon adhesion to collagen (Figure 5C), as were formation of procoagulant platelets, α-granule release and integrin activation, measured by Annexin-V-647, anti-P-selectin-FITC and JON/A-PE antibody binding, respectively (Figure 5B, C). Interestingly, *G6b-B diY/F* platelet αIIbβ3 activation on vWF-BP-laminin-rhodocytin was unaltered, whilst it was reduced in *G6b KO* samples. This could indicate a residual function of G6b-B, independent of Shp1 and Shp2 interactions. Previous studies using human blood showed an effect of low platelet counts on adhesion and activation in this assay, particularly on collagen-coated surfaces.[16] The observed reductions are therefore at least partially due to thrombocytopenia in the *loss-of-function* and *KO* models.

Collectively, evidence from the *in vitro* and *ex vivo* assays demonstrate that a combination of reduced platelet counts and defective activation responses produce the hemostatic defect observed in *G6b-B diY/F* mice (Figure 3A). The combination of platelet defects is likely also responsible for the bleeding symptoms identified in *G6b loss-of-function* patients (Hofmann *et al*, co-submitted).

G6b-B inhibits CLEC-2 signaling via Shp2

Since ITIM-containing receptors are most commonly characterized as negative regulators of ITAM-containing receptor signaling, we set out to determine at which stage G6b-B targets this pathway in platelets. The increased aggregation response to anti-CLEC-2 antibody in *G6b-B diY/F* mice (Figure 4A) made this hemi-ITAM-containing receptor ideal for further investigation. Washed platelets from *G6b KO*, *G6b-B diY/F*, *Shp1 KO* and *Shp2 KO,* and *WT* mice, were activated with 10 μg/mL anti-CLEC-2 antibody for three minutes. Key

proximal tyrosine phosphorylation signaling events were then assessed by western blotting (Figure 6). As expected from aggregation studies (Figure 4A),[6,12] platelets from *G6b KO*, *G6b-B diY/F* and *Shp2 KO* mice all exhibited increased whole cell tyrosine phosphorylation (p-Tyr) following antibody-mediated CLEC-2 stimulation, compared to *WT* platelets (Figure 6A, B, C). Platelets from the *Shp1 KO* mice did not (Figure 6D),[12] suggesting G6b-B mediates an inhibitory effect on CLEC-2 signaling through Shp2 specifically. Rhodocytin-mediated tyrosine phosphorylation in *G6b-B diY/F* platelets was normal (Figure S8), correlating with the normal aggregation and ATP secretion responses (Figure 4A).

Using phospho-specific antibodies, we investigated the site of action of G6b-B-Shp2 on CLEC-2 signaling. We focused on SFKs, which phosphorylate the tyrosine residue within the hemi-ITAM of the CLEC-2 receptor, and spleen tyrosine kinase (Syk), which binds the phosphorylated hemi-ITAMs of two adjacent CLEC-2 receptors and mediates downstream effects. SFK activation was indirectly measured as *trans*-autophosphorylation of the highly conserved tyrosine residue 418 in Src (Src p-Tyr418) and Syk activation as *trans*-autophosphorylation of tyrosine residues 519/520 (p-Tyr519/20), both of which directly correlate with activity. Following quantification, Src p-Tyr418 was not significantly altered in CLEC-2-stimulated platelets from all mouse models, whereas Syk p-Tyr519/520 was significantly higher in CLEC-2-stimulated *G6b KO*, *G6b-B diY/F* and *Shp2 KO* compared with *WT* and *Shp1 KO* platelets (Figure 6A-D). It should be noted that co-migrating plasma proteins present in both *G6b KO* and *G6b-B diY/F* samples occasionally interfered with the migration and appearance of Syk blots. This was controlled for when quantifying by normalizing Syk p-Tyr519/20 band intensities to total Syk band intensities for each sample. These findings suggest that G6b-B-Shp2 inhibits CLEC-2 signaling by directly dephosphorylating either CLEC-2, to abolish Syk association, and/or Syk, attenuating its activity.

Shp2 interacts directly with phosphorylated G6b-B in an extended orientation

Since Shp2 appears to be the dominant mediator of G6b-B function in mouse platelets,[12] and the proteins are known to associate by co-immunoprecipitation and direct phosphopeptide binding experiments,[6,10,17] we investigated the structural basis of their interaction in solution using heteronuclear magnetic resonance (NMR) spectroscopy. Recombinant N- and C-SH2 domains of Shp2 were incubated with phospho-peptides corresponding to the ITIM (p-ITIM) and ITSM (p-ITSM) of G6b-B. This revealed that the N- and C-SH2 domains of Shp2 preferentially interact with p-ITIM and p-ITSM of G6b-B, respectively (Figure 7A, B). The chemical shift perturbations between apo and bound forms of C-SH2 and p-ITSM exhibited slow exchange, indicating strong interactions. This accounts for the increased affinity of the tandem SH2 domain for the dual p-ITIM and p-ITSM peptide, over that seen with isolated N-SH2.[17] The tandem SH2-phospho-peptide interaction showed comparable chemical shift perturbations, indicating synergistic binding of the doubly phosphorylated peptide to both SH2 domains (Figure 7C, D). The direct interaction of Shp2 SH2 domains with G6b-B cognate binding motifs explains the critical role of the two residues mutated in the *G6b-B diY/F* mice reported here. Moreover, the structural model of the complex is fully supported by earlier studies reporting the binding affinity to be 0.5 nM.[17] The structural studies show that the Y/F substitutions would eliminate critical contacts that allow the deep, simultaneous insertion of G6b-B's ITIM and ITSM phosphotyrosine residues into Shp2 N-SH2 and C-SH2 domains, respectively, in a manner that is consistent with canonical SH2 ligand binding modes.[18] Moreover, the interaction with Shp2 tandem SH2 domains would also be compromised by G6b-B deletions and point mutations in Shp2, including L210I, R223H/C and A238V that have been found in human tumors,[19-21] suggesting wider roles for Shp2 uncoupling in cancer.

Discussion

This study establishes the physiological significance of tyrosine phosphorylation of the ITIM and ITSM domains of G6b-B in regulating platelet number and function. Uncoupling of G6b-B from Shp1 and Shp2 leads to a severe platelet phenotype, closely resembling that observed in G6b-B-deficient mice and patients (*Hofmann et al. co-submitted*).[6] The primary features of the G6b-B *loss-of-function* and *KO* phenotypes included severe macrothrombocytopenia due to reduced platelet production, large MK clusters and myelofibrosis at sites of hematopoiesis, down-regulation of the GPVI-FcR-γ-chain complex and increased signaling through CLEC-2 in platelets. Increased platelet activation via the CLEC-2 pathway was specifically due to Shp2 recruitment to G6b-B, which acted to inhibit the hemi-ITAM-Syk dependent pathway.

Minor differences in the phenotypes of *G6b diY/F KI* and *KO* mouse models may be due to residual functions of G6b-B diY/F, a dominant negative effect of this mutant form of the receptor or functional roles of splice isoforms of G6b-B, which have been hypothesized to exist. Despite the apparent difference in bleeding between *G6b-B diY/F KI* and *KO* mice, this did not reach significance. Potential incomplete penetrance of the *G6b-B diY/F* phenotype correlates with an identified null patient presenting with no clinical symptoms (*Hofmann et al., co-submitted*). However, variability in humans beyond *G6b* mutations could explain the observed differences between patients.

We previously reported a strong overlap between the phenotype of *Shp1/2 DKO* mice and *G6b conditional KO* (*G6b*$^{fl/fl}$*; Pf4-Cre*$^{+}$) mice.[12] However, the phenotype of *Shp1/2 DKO* mice was more severe than that of *G6b conditional KO* mice, including severe developmental defects in MKs that were not observed in G6b-B-deficient mice, reflecting other functional roles of Shp1 and Shp2. Thus, the *G6b-B diY/F KI* mouse model provides a more refined approach to demonstrate that G6b-B signals exclusively through Shp1 and

Shp2. This G6b-B *loss-of-function* mouse model also allows for expression of other splice isoforms of G6b-B. This includes G6b-A-like, which is predicted to share the same extracellular, transmembrane and juxtamembrane regions as G6b-B, but has an entirely different cytoplasmic tail, lacking the ITIM and ITSM. Although we have demonstrated expression of the G6b-A splice variant in human platelets, using a custom anti-G6b-A antibody (*Hofmann et al. co-submitted*), generation of an antibody specific to the mouse G6b-A-like protein has been unsuccessful. This is due to lack of antigenic sites in the predicted mouse G6b-A-like protein. The function of human G6b-A also remains unknown, but advances can now be made through the use of the custom antibody and humanized *G6b* mouse model described by *Hofmann et al.* (*co-submitted*).

G6b-B appears to primarily signal through Shp2 in mice, as *Shp2 KO* mice more closely phenocopied *G6b KO* and *G6b-B diY/F* mice than *Shp1 KO* mice.[12] This may be accounted for by the affinity of Shp2 for G6b-B being 100-fold greater than Shp1,[17] and/or the relative stoichiometry of the two PTPs. Shp2 is expressed at levels six-fold greater than Shp1 in mouse platelets,[22] meaning in the absence of Shp1, the highly expressed Shp2 may provide better compensation than *vice versa*. Structural characterization of Shp2 modular interaction with phospho-G6b-B-ITIM-ITSM peptides revealed simultaneous binding of its N-SH2 domain with the phospho-ITIM and its C-SH2 domain with the phospho-ITSM, resulting in a high affinity interaction that is dependent on the phosphotyrosines that were substituted in the knock-in mice. This double mutation would compromise the complexed orientation that alleviates the intra-molecular interaction, between the backside of the N-SH2 domain of Shp2 and the PTP catalytic site, that normally allows activation of the phosphatase.[11] Moreover, the double mutation would have prevented the high affinity, stable interaction with G6b-B that provides localization of Shp2

to the plasma membrane, with its PTP domain freely available for engagement with substrates, including phosphorylated CLEC-2 and/or Syk.

One of the main phenotypes of the *G6b-B diY/F* mouse is the severe macrothrombocytopenia, which was found to be due to reduced platelet production, and not increased clearance. Comparison of the proportionate slopes of reduction in biotinylated platelets in circulation showed no significant difference with *WT* mice, which does not correlate with increased clearance of *G6b KO* platelets previously published.[6] However, this most likely reflects the method of analysis, as the total platelet counts are not significantly different. Reduced platelet counts are therefore due to decreased platelet production, supported by the reduced platelet recovery following depletion and observed extramedullary hematopoiesis.

Analysis of the regulation of ITAM-containing receptor signaling by G6b-B in the *G6b-B diY/F* mouse model is complicated by the reduced platelet counts and severe down-regulation of the collagen receptor complex GPVI-FcRγ. This down-regulation of GPVI-FcRγ is thought to be due to loss of inhibition of Syk, by G6b-B recruited Shp1 and Shp2, activating negative feedback mechanisms, such as shedding.[6] Both flow cytometric and lumi-aggregometry based assays showed reduced *G6b-B diY/F* response to GPVI-specific agonists. The predicted increase in signaling in the absence of G6b-B-Shp1-Shp2 interaction is therefore not sufficient to overcome the down-regulation of GPVI.

In contrast, flow cytometry, aggregation and biochemical studies showed the expected hyper-reactivity of *G6b-B diY/F* platelets to CLEC-2-mediated hemi-ITAM signaling. Similar increases in signaling were observed in *G6b KO* and *Shp2 KO*, but not in *Shp1 KO* mice. Syk, and not SFK, activation was increased in these mice indicating Syk, and/or the CLEC-2 receptor itself, are the target of G6b-B-Shp2 phosphatase activity. The pathophysiological consequences of increased CLEC-2 activity is presently not known and

cannot be ascertained using either the *G6b KO* or *G6b diY/F* mouse models due to the concomitant reductions in platelet counts and accompanying platelet anomalies. Thus, other means of investigating effects of increased CLEC-2 signaling on vessel development, permeability and other physiological processes will have to be implemented.

Other than in washed platelets stimulated with CLEC-2 antibody, P-selectin exposure was significantly reduced in response to all agonists. Absence of α-granule release rescue upon PAR4p and ADP co-stimulation indicate that defects are not due to loss of secondary signaling.[23] Together with the reduced spreading, this suggests a positive regulatory role for G6b-B in regulating α-granule release. Interestingly, agonists that activate G protein-coupled receptors (GPCRs) also showed attenuated aggregation responses in *G6b-B diY/F* mouse platelets. This may indicate direct involvement of the G6b-B-Shp1-Shp2 signaling complex in regulation of GPCR-mediated tyrosine kinase signaling,[24,25] or an indirect consequence of other platelet defects, including aberrant secretion or receptor turnover. The regulation of GPCR signaling by ITIM-containing receptors is highly provocative and warrants further investigation.

Despite *Shp2 KO* mice most closely resembling *G6b KO* and *G6b-B diY/F* phenotypes, some features do not overlap.[12,13] *Shp1 KO* mice show normal platelet production, clearance and reactivity to most agonists. However, the absence of Shp1 in platelets reduces GPVI surface expression, as observed in *G6b-B diY/F* platelets. Platelets from both models are therefore hypo-responsive to GPVI-specific activation. GPVI is known to be shed from the platelet surface once activated,[26] indicating that loss of G6b-B-Shp1 mediated inhibition causes activation of this negative feedback mechanism.

These findings confirm the hypothesis that the regulation of platelet homeostasis by G6b-B is dependent upon recruitment and signal transduction by the PTPs Shp1 and Shp2. Loss of this interaction severely impairs the formation of functional platelets that are

essential for the maintenance of hemostasis. As GPVI and CLEC-2 share common downstream signaling proteins, it is of note that they are differentially regulated by Shp1 and Shp2.[12] Whether this is due to differences in compartmentalized recruitment of Shp1 and Shp2 into proximity with GPVI and CLEC-2, which may be localized differentially in the plasma membrane, or differences in targeting of proteins specific to each pathway, remains to be determined.

Acknowledgements

M.J.G. is funded by a Medical Research Council PhD studentship (GBT1564), A.M. is a BHF Intermediate Basic Science Research Fellow (FS/15/58/31784) and Y.A.S. is a BHF Senior Basic Science Research Fellow (FS/13/1/29894). P.G. was funded by Cancer Research UK, M.J. by the BBSRC, and M.O. received Bloodwise and Cancer Research UK support. HWB-NMR provided NMR facility access through Wellcome Trust support. Rhodocytin was purified as part of the project financed by Deutsche Forschungsgemeinschaft (DFG grant EB177/13-1). We would like to thank Inga Hofmann (University of Wisconsin, USA) and Mark Fleming (Boston Children's Hospital, USA) for interpretation of mouse pathology and constructive feedback on the manuscript.

Authorship Contributions

M.J.G. – performed experiments, analyzed data, wrote and revised the manuscript

J.P.V.G. – performed experiments, analyzed data, revised the manuscript

P.G. – performed experiments, analyzed data, revised the manuscript

T.V. – performed experiments, analyzed data, revised the manuscript

C.W.S. – performed experiments, analyzed data, revised the manuscript

S.H. – performed experiments, analyzed data

M.J.E.K. – performed experiments, analyzed data

B.M.E.T. – analyzed data

G.E.J. – analyzed data, revised the manuscript

J.A.E. - supply of essential reagents

M.J. – performed experiments, analyzed data, revised the manuscript

M.O. – revised the manuscript, contributed intellectually

J.W.M.H. – performed experiments, analyzed data, revised the manuscript

A.M. – designed experiments, interpreted data, wrote and revised the manuscript

Y.A.S. – conceptualized, analyzed data, wrote and revised the manuscript

Conflict-of-interest disclosure

The authors have no competing financial interests to declare.

References

1. George JN. Platelets. *Lancet*. 2000;355(9214):1531-1539.
2. Hartwig JH. The platelet: form and function. *Semin Hematol*. 2006;43(1 Suppl 1):S94-100.
3. Coxon CH, Geer MJ, Senis YA. ITIM receptors: more than just inhibitors of platelet activation. *Blood*. 2017;129(26):3407-3418.
4. Daëron M, Jaeger S, Pasquier L, Vivier E. Immunoreceptor tyrosine-based inhibition motifs: a quest in the past and future. *Immunol Rev*. 2008;224:11-43.
5. Cannons JL, Tangye SG, Schwartzberg PL. SLAM family receptors and SAP adaptors in immunity. *Annu Rev Immunol*. 2011;29:665-705.
6. Mazharian A, Wang YJ, Mori J, et al. Mice lacking the ITIM-containing receptor G6b-B exhibit macrothrombocytopenia and aberrant platelet function. *Sci Signal*. 2012;5(248):ra78.
7. Washington AV, Gibot S, Acevedo I, et al. TREM-like transcript-1 protects against inflammation-associated hemorrhage by facilitating platelet aggregation in mice and humans. *J Clin Invest*. 2009;119(6):1489-1501.
8. Fan X, Shi P, Dai J, et al. Paired immunoglobulin-like receptor B regulates platelet activation. *Blood*. 2014;124(15):2421-2430.
9. Melhem M, Abu-Farha M, Antony D, et al. Novel G6B gene variant causes familial autosomal recessive thrombocytopenia and anemia. *Eur J Haematol*. 2017;98(3):218-227.
10. Senis YA, Tomlinson MG, Garcia A, et al. A comprehensive proteomics and genomics analysis reveals novel transmembrane proteins in human platelets and mouse megakaryocytes including G6b-B, a novel immunoreceptor tyrosine-based inhibitory motif protein. *Mol Cell Proteomics*. 2007;6(3):548-564.
11. Hof P, Pluskey S, Dhe-Paganon S, Eck MJ, Shoelson SE. Crystal structure of the tyrosine phosphatase SHP-2. *Cell*. 1998;92(4):441-450.
12. Mazharian A, Mori J, Wang YJ, et al. Megakaryocyte-specific deletion of the protein-tyrosine phosphatases Shp1 and Shp2 causes abnormal megakaryocyte development, platelet production, and function. *Blood*. 2013;121(20):4205-4220.
13. Di Paola J. SHPing in different directions in platelet production. *Blood*. 2013;121(20):4018-4019.
14. Morowski M, Vogtle T, Kraft P, Kleinschnitz C, Stoll G, Nieswandt B. Only severe thrombocytopenia results in bleeding and defective thrombus formation in mice. *Blood*. 2013;121(24):4938-4947.
15. Pollitt AY, Grygielska B, Leblond B, Desire L, Eble JA, Watson SP. Phosphorylation of CLEC-2 is dependent on lipid rafts, actin polymerization, secondary mediators, and Rac. *Blood*. 2010;115(14):2938-2946.
16. Nagy M, Mastenbroek TG, Mattheij NJA, et al. Variable impairment of platelet functions in patients with severe, genetically linked immune deficiencies. *Haematologica*. 2018;103(3):540-549.
17. Coxon CH, Sadler AJ, Huo J, Campbell RD. An investigation of hierachical protein recruitment to the inhibitory platelet receptor, G6B-b. *PLoS One*. 2012;7(11):e49543.
18. Gopalasingam P, Quill L, Jeeves M, Overduin M. SH2 Domain Structures and Interactions. In: Kurochkina N, ed. SH Domains: Structure, Mechanisms and Applications. Cham: Springer International Publishing; 2015:159-185.
19. Giannakis M, Mu XJ, Shukla SA, et al. Genomic Correlates of Immune-Cell Infiltrates in Colorectal Carcinoma. *Cell Rep*. 2016.
20. Comprehensive genomic characterization of squamous cell lung cancers. *Nature*. 2012;489(7417):519-525.
21. Cerami E, Gao J, Dogrusoz U, et al. The cBio cancer genomics portal: an open platform for exploring multidimensional cancer genomics data. *Cancer Discov*. 2012;2(5):401-404.
22. Zeiler M, Moser M, Mann M. Copy number analysis of the murine platelet proteome spanning the complete abundance range. *Mol Cell Proteomics*. 2014;13(12):3435-3445.
23. Harper MT, van den Bosch MT, Hers I, Poole AW. Platelet dense granule secretion defects may obscure alpha-granule secretion mechanisms: evidence from Munc13-4-deficient platelets. *Blood*. 2015;125(19):3034-3036.

24. Dorsam RT, Kim S, Murugappan S, et al. Differential requirements for calcium and Src family kinases in platelet GPIIb/IIIa activation and thromboxane generation downstream of different G-protein pathways. *Blood*. 2005;105(7):2749-2756.
25. Canobbio I, Cipolla L, Guidetti GF, et al. The focal adhesion kinase Pyk2 links Ca2+ signalling to Src family kinase activation and protein tyrosine phosphorylation in thrombin-stimulated platelets. *Biochem J*. 2015;469(2):199-210.
26. Gardiner EE, Andrews RK. Platelet receptor expression and shedding: glycoprotein Ib-IX-V and glycoprotein VI. *Transfus Med Rev*. 2014;28(2):56-60.

Figure legends

Figure 1. Loss of ITIM/ITSM phosphorylation prevents G6b-B-Shp1-Shp2 interaction.

(A) Flow cytometric and (B) western blot analysis of G6b-B expression in platelets from *WT* and *G6b-B diY/F* mice. Mean ± SEM (n=6) of G6b-FITC median fluorescence intensity, with rat IgG2A subtracted. Representative blots and quantification, normalized to tubulin reblots (mean ± SEM, n=3). (C) Lysates were prepared using washed platelets (5 × 10^8/mL) under basal and 30 μg/mL collagen stimulated conditions (90 seconds, 37ºC, stirring at 1200 rpm) from *WT* and *G6b-B diY/F* mice. Co-immunoprecipitation of Shp1 and Shp2 was investigated by western blotting, following immunoprecipitation using anti-G6b-B or non-immune rabbit polyclonal antibodies.

Figure 2. Uncoupling of G6b-B-Shp1-Shp2 disrupts platelet production

(A) Percentage of reticulated platelets following staining with ReticCount, mean ± SEM (n=6), ***$P < 0.001$. (B) Clearance of platelets in *WT* and *G6b-B diY/F* mice, following labelling with I.V. injected NHS-biotin. Biotin labelled platelets measured by Streptavidin-PE binding in tail vein-sampled whole blood, mean ± SEM, n=5-6 per data point. Rate of platelet elimination calculated from slope of loss of biotinylated platelets, mean ± SEM, n=6. (C) Platelet recovery following anti-GPIbα antibody mediated platelet depletion in *WT* and *G6b-B diY/F* mice (n=8-20 per time point). Platelet recovery rate calculated from recovery data for *WT* and *G6b-B diY/F* mice between days 3 and 7, mean ± SEM, n=8-11, ***$P < 0.001$. (D) Representative images and quantification of the number of megakaryocytes in H&E stained spleen and femur sections from *WT* and *G6b-B diY/F* mice, mean ± SEM, n=6 mice, 5 images per mouse, ***$P < 0.001$. Yellow arrow heads indicated megakaryocytes. Representative images of reticulin staining showing myelofibrosis of *WT* and *G6b-B diY/F* spleens and femurs (scale bar: 50 μm). Spleen to body weight ratio in *WT*, *G6b-B diY/F* and *G6b KO*, mean ± SEM, n=22, ***$P < 0.001$.

Figure 3. Aberrant platelet activation in *G6b-B diY/F* mice

(A) Blood loss to body weight ratio following excision of 5 mm of tail tip in isofluorane anaesthetized mice of the indicated genotypes. Data was analyzed using a bi-modal function, comprising of a gamma and normal distribution for low and high bleeding tendency, respectively. Likelihood ratio tests were performed to determine whether the probability of bleeding (P_{bleed}) differed between genotypes. (A, B, C, D) Flow cytometric measurement of P-selectin exposure and fibrinogen binding of *WT* and *G6b-B diY/F* platelets in whole blood using (A) Immunoreceptor tyrosine-based activation motif-activating and (B) G protein-coupled receptor-activating agonists, mean ± SEM, n=5-6 per stimulation. Thrombin stimulations were in the presence of 10 μM GPRP to prevent blood clotting. (C) Rescue of activating PAR4 peptide (PAR4p) stimulated fibrinogen binding in the presence of 10 μM ADP, mean ± SEM, n=5-6. Platelets were gated using forward- and side-scatter and 10,000 events collected.

Figure 4. Aberrant platelet function in *G6b-B diY/F* mice

(A) Mean aggregation and ATP release traces in washed platelets (2×10^8/mL). For ADP aggregations, platelets were washed in the presence of 0.02 U/mL apyrase and supplemented with 1 μM $CaCl_2$ and 50 μg/mL fibrinogen. Mean ± SEM, n=4-5. (B) Representative images of *WT* and *G6b-B diY/F* washed platelet (2×10^7/mL) spreading on fibrinogen under basal and 0.1 U/mL thrombin preactivated conditions (scale bar: 5 μm). Quantification of surface area coverage (***P < 0.001), platelet perimeter (n.s.), total platelets per image (n.s.) and four stages of spreading in the presence of thrombin (***P < 0.001), mean ± SEM, n=5-6.

Figure 5. Reduced platelet adhesion and activation under flow conditions.

PPACK, heparin and fragmin anticoagulated whole blood from *WT*, *G6b-B diY/F* and *G6b KO* mice was flowed for 3.5 minutes, 1000 s^{-1} shear, over coverslips coated with collagen, von Willebrand Factor-binding protein (vWF-BP) + laminin and vWF-BP + laminin + rhodocytin. (A) Representative brightfield images, (B) representative fluorescence images following staining with Alexa-647 conjugated annexin V, P-selectin-FITC and JON/A-PE antibodies to measure phosphatidylserine positive platelets, α-granule release and αIIbβ3 integrin activation (αIIb$\beta3^{act}$), respectively (scale bar: 10 μm). (C) Heatmap to show effect size of morphology scores and surface area coverage (SAC) of indicated parameters, normalized to *WT* (n=5-6).

Figure 6. G6b-B-Shp2 regulates CLEC-2 signaling.

Washed platelets (4 × 10^8/mL) from (A) *G6b KO*, (B) *G6b-B diY/F*, (C) *Shp1 KO* and (D) *Shp2 KO* mice, and litter matched *WT* controls, were activated with 10 μg/mL of activating CLEC-2 antibody in the presence of 10 μM lotrafiban, before lysing and investigation of named phospho-tyrosine sites by western blotting. Representative western blots from three independent experiments.

Figure 7. Structural basis of G6b-B recognition by SHP2

The specific interactions are shown by comparison of (A) N-SH2 apo (black) and N-SH2 + 1 equivalent pITIM (sky blue) (B) C-SH2 apo (black) and C-SH2 + 1 equivalent pITSM (red) and (C) tandem SH2 apo (teal) and tandem SH2 + 1 equivalent pITIM+pITSM (red). Selected chemical shift perturbations in SOFAST-HMQC NMR spectra are labeled. (D) Lowest energy model of tandem SH2 bound to pITIM+pITSM generated by HADDOCK based on restraints generated from the NMR data. Residues showing large chemical shift perturbations are shown in blue and are defined as active residues directly involved in

interaction with the peptide. Residues showing small yet significant chemical shift perturbations are shown in cyan and are defined as passively involved residues.

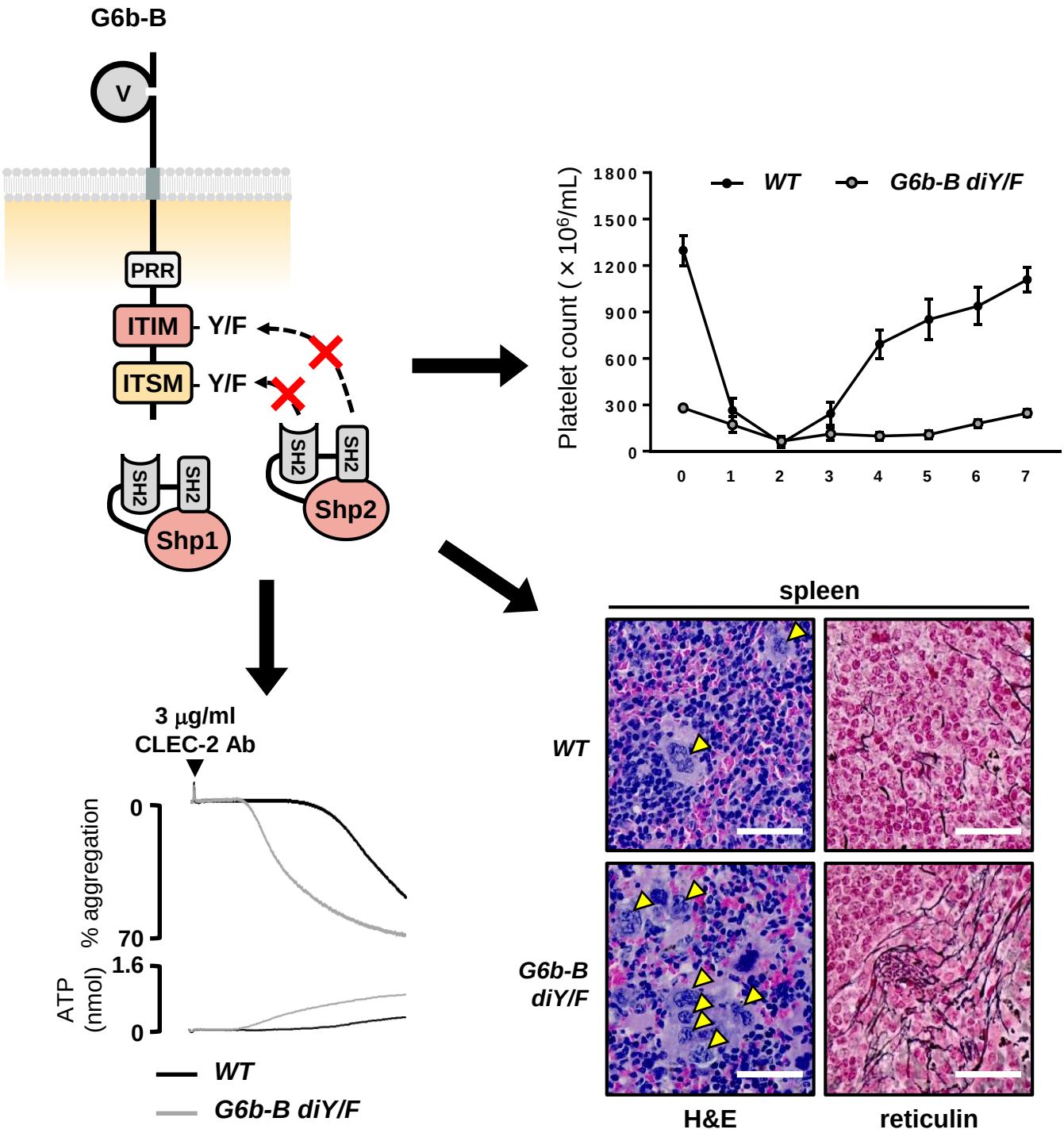
G6b-B
V
PRR
ITIM
Y/F
ITSM
Y/F
SH2
SH2
Shp1
SH2
SH2
Shp2
Platelet count (× 10⁶/mL)
1800
1500
1200
900
600
300
0
0
1
2
3
4
5
6
7
WT
G6b-B diY/F
3 μg/ml
CLEC-2 Ab
% aggregation
0
70
ATP
(nmol)
1.6
0
WT
G6b-B diY/F
spleen
WT
G6b-B
diY/F
H&E
reticulin

Figure 1

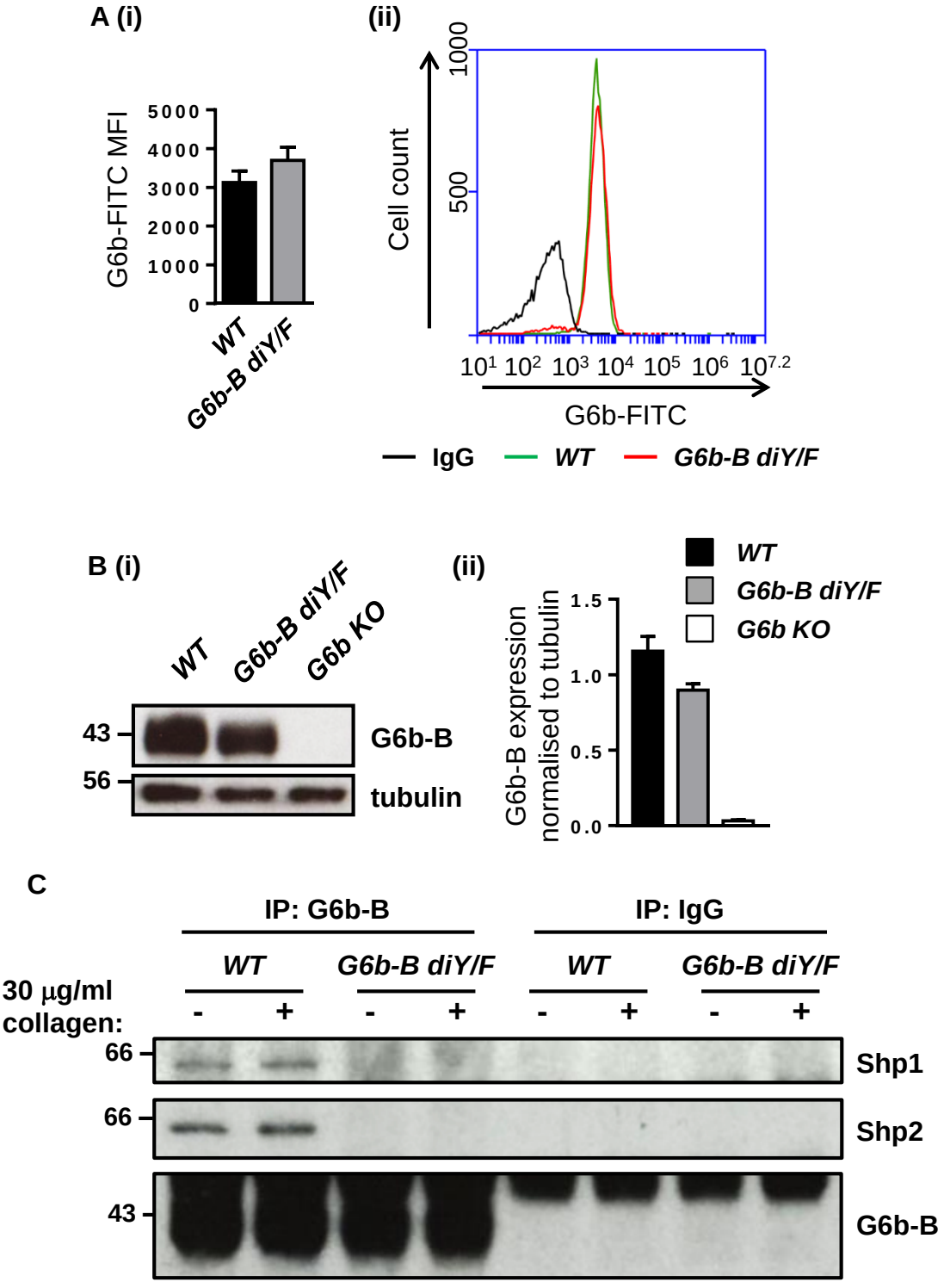
A (i)
G6b-FITC MFI
5000
4000
3000
2000
1000
0
WT
G6b-B diY/F
(ii)
Cell count
1000
500
10¹ 10² 10³ 10⁴ 10⁵ 10⁶ 10⁷.²
G6b-FITC
IgG
WT
G6b-B diY/F
B (i)
WT
G6b-B diY/F
G6b KO
43
56
G6b-B
tubulin
(ii)
WT
G6b-B diY/F
G6b KO
G6b-B expression normalised to tubulin
1.5
1.0
0.5
0.0
C
IP: G6b-B
IP: IgG
WT
G6b-B diY/F
WT
G6b-B diY/F
30 μg/ml collagen:
- + - + - + - +
66
Shp1
66
Shp2
43
G6b-B

Figure 2

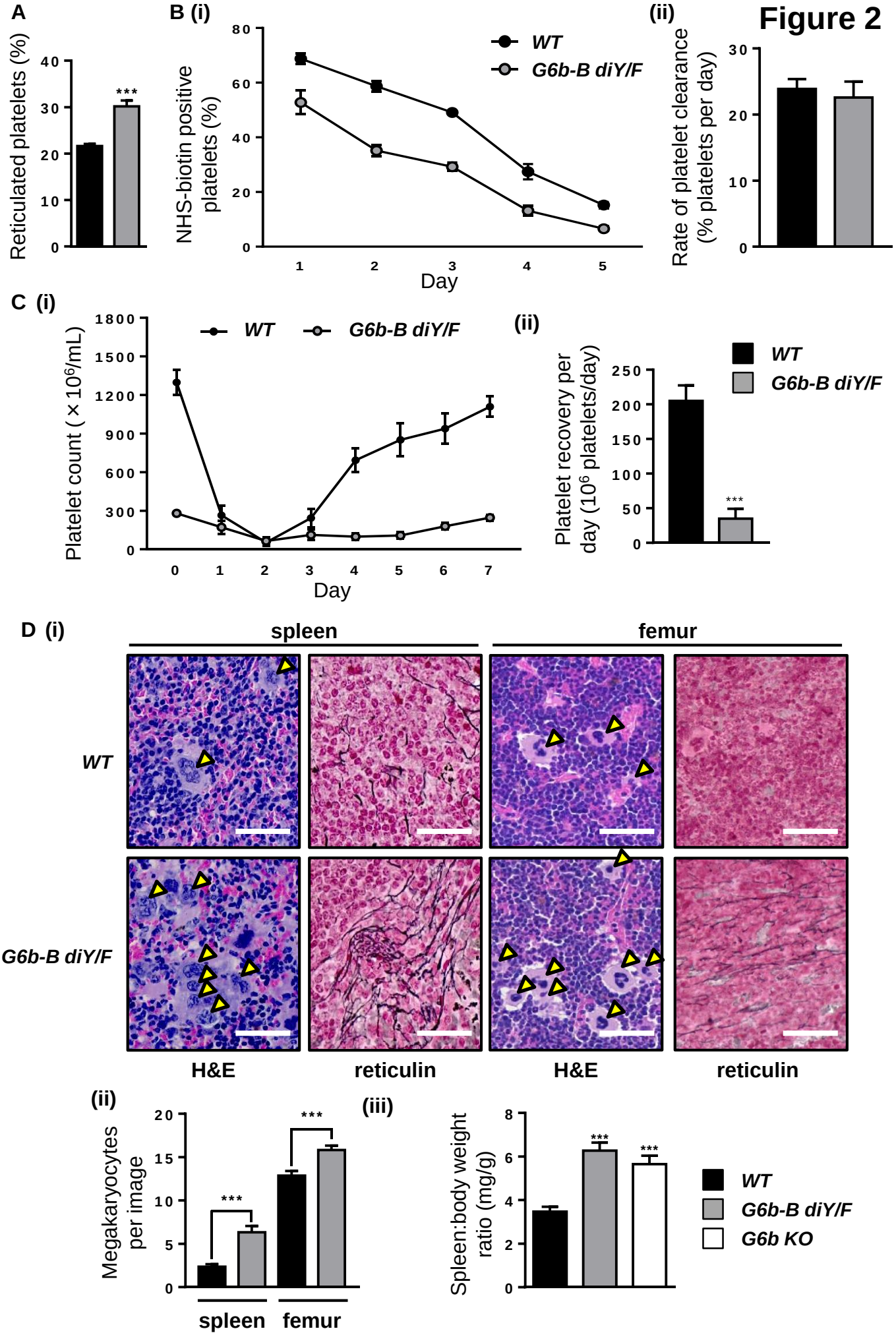
A
Reticulated platelets (%)
***
B (i)
NHS-biotin positive platelets (%)
WT
G6b-B diY/F
Day
(ii)
Rate of platelet clearance (% platelets per day)
C (i)
Platelet count (× 10⁶/mL)
WT
G6b-B diY/F
Day
(ii)
Platelet recovery per day (10⁶ platelets/day)
WT
G6b-B diY/F
***
D (i)
spleen
femur
WT
G6b-B diY/F
H&E
reticulin
H&E
reticulin
(ii)
Megakaryocytes per image
***
***
spleen
femur
(iii)
Spleen:body weight ratio (mg/g)
***
***
WT
G6b-B diY/F
G6b KO

Figure 3

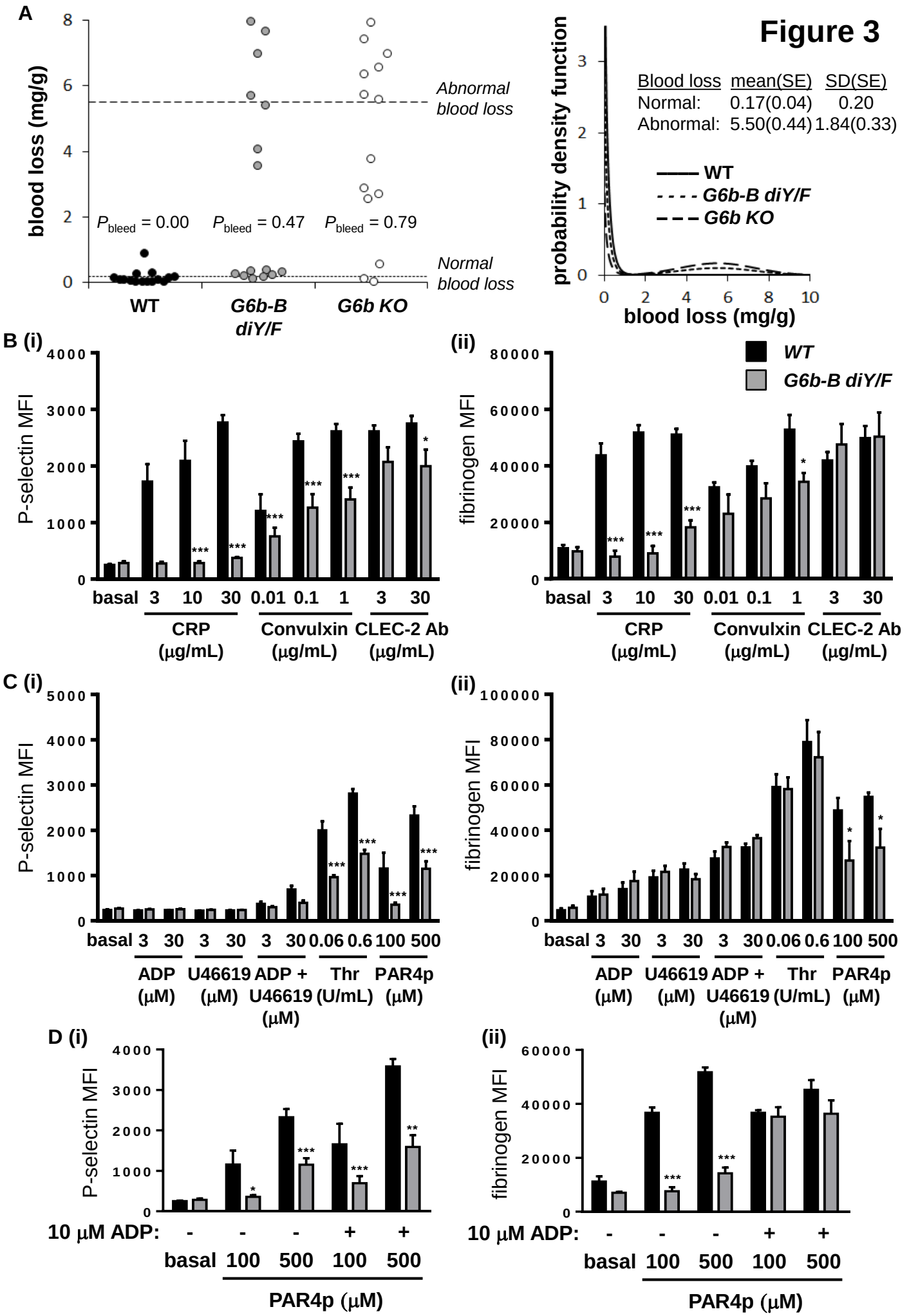
A
blood loss (mg/g)
Abnormal blood loss
Normal blood loss
P_{bleed} = 0.00
P_{bleed} = 0.47
P_{bleed} = 0.79
WT
G6b-B diY/F
G6b KO
probability density function
Blood loss mean(SE) SD(SE)
Normal: 0.17(0.04) 0.20
Abnormal: 5.50(0.44) 1.84(0.33)
WT
G6b-B diY/F
G6b KO
blood loss (mg/g)
B (i)
P-selectin MFI
(ii)
fibrinogen MFI
WT
G6b-B diY/F
basal 3 10 30 0.01 0.1 1 3 30
CRP (μg/mL)
Convulxin (μg/mL)
CLEC-2 Ab (μg/mL)
C (i)
P-selectin MFI
(ii)
fibrinogen MFI
basal 3 30 3 30 3 30 0.06 0.6 100 500
ADP (μM)
U46619 (μM)
ADP + U46619 (μM)
Thr (U/mL)
PAR4p (μM)
D (i)
P-selectin MFI
(ii)
fibrinogen MFI
10 μM ADP: - - - + +
basal 100 500 100 500
PAR4p (μM)

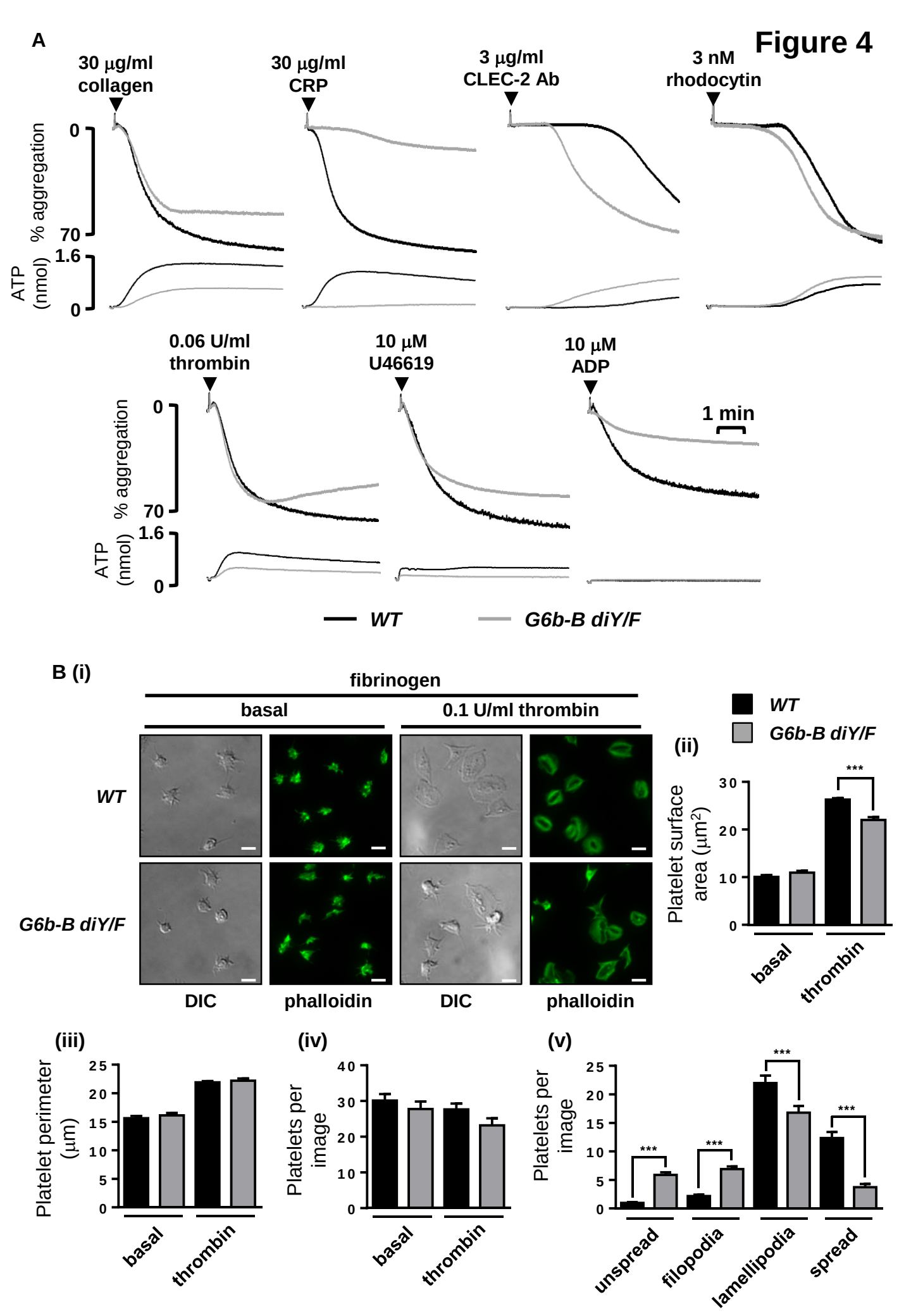
Figure 4
A
30 μg/ml collagen
30 μg/ml CRP
3 μg/ml CLEC-2 Ab
3 nM rhodocytin
% aggregation
0
70
ATP (nmol)
1.6
0
0.06 U/ml thrombin
10 μM U46619
10 μM ADP
1 min
WT
G6b-B diY/F
B (i)
fibrinogen
basal
0.1 U/ml thrombin
WT
G6b-B diY/F
DIC
phalloidin
DIC
phalloidin
(ii)
Platelet surface area (μm²)
basal
thrombin
(iii)
Platelet perimeter (μm)
basal
thrombin
(iv)
Platelets per image
basal
thrombin
(v)
Platelets per image
unspread
filopodia
lamellipodia
spread

Figure 5

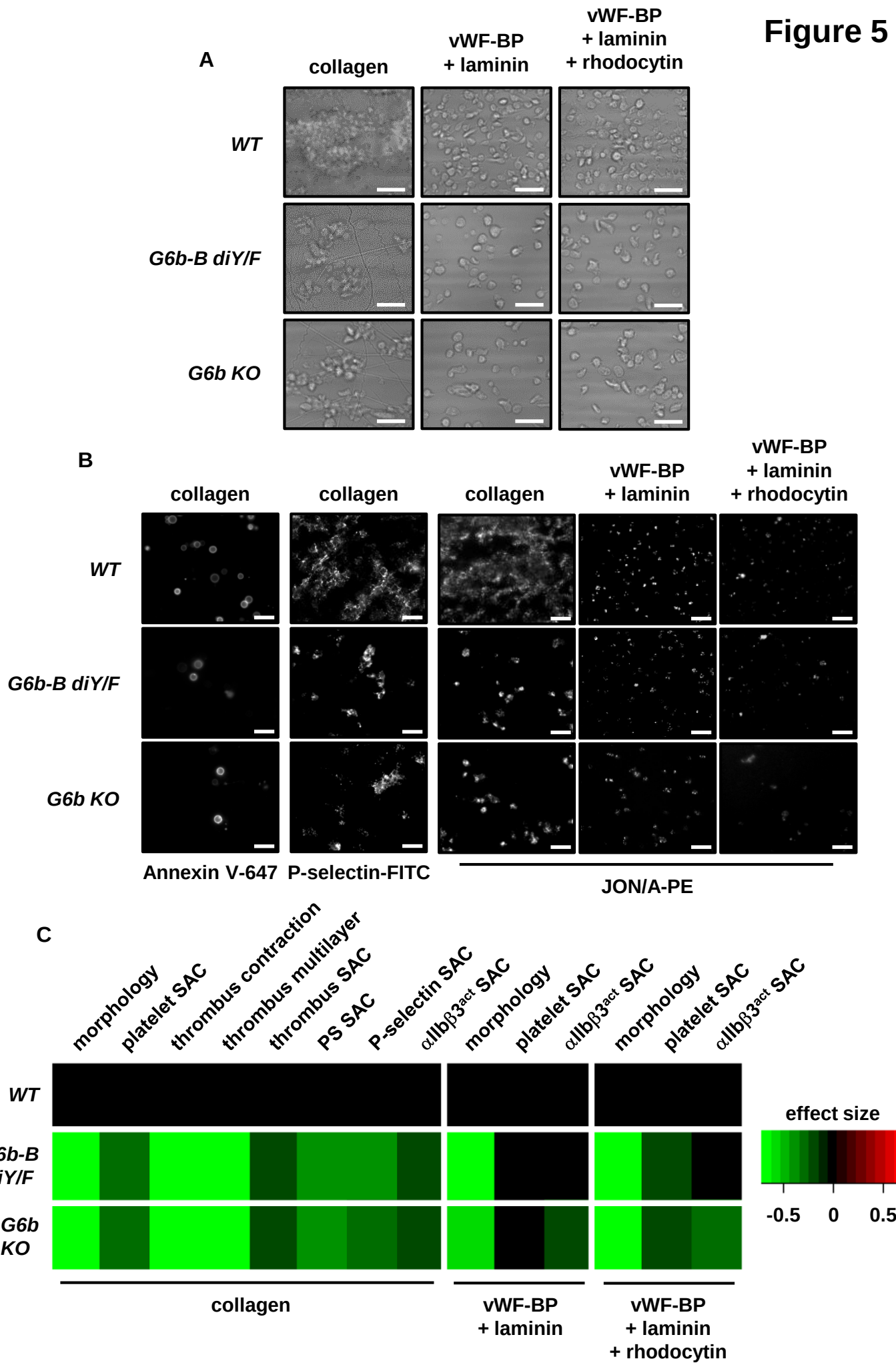
A
collagen
vWF-BP + laminin
vWF-BP + laminin + rhodocytin
WT
G6b-B diY/F
G6b KO
B
collagen
collagen
collagen
vWF-BP + laminin
vWF-BP + laminin + rhodocytin
WT
G6b-B diY/F
G6b KO
Annexin V-647
P-selectin-FITC
JON/A-PE
C
morphology
platelet SAC
thrombus contraction
thrombus multilayer
thrombus SAC
PS SAC
P-selectin SAC
αIIbβ3act SAC
morphology
platelet SAC
αIIbβ3act SAC
morphology
platelet SAC
αIIbβ3act SAC
WT
G6b-B diY/F
G6b KO
effect size
-0.5
0
0.5
collagen
vWF-BP + laminin
vWF-BP + laminin + rhodocytin

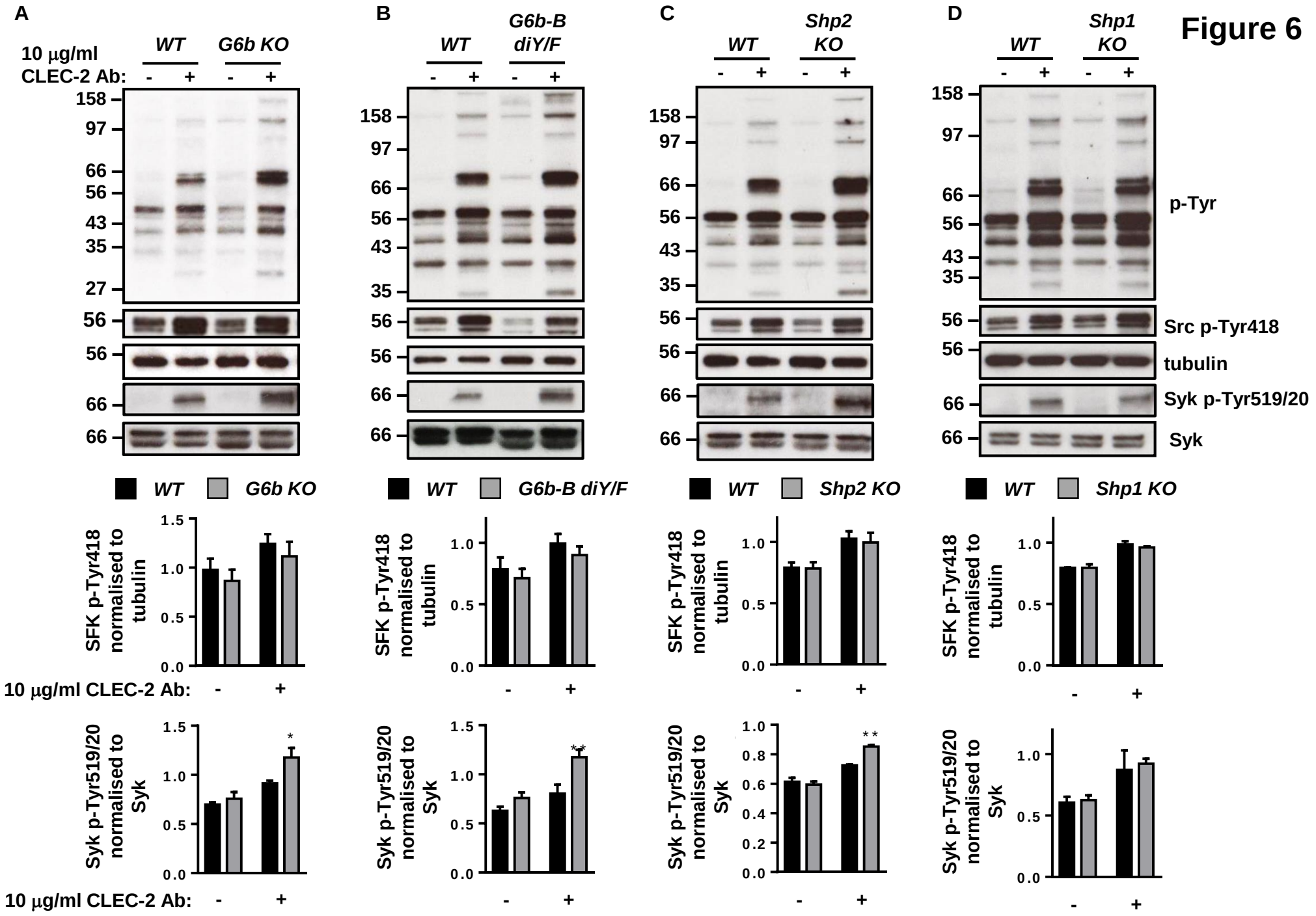
A
B
C
D
Figure 6
10 μg/ml CLEC-2 Ab:
WT
G6b KO
G6b-B diY/F
Shp2 KO
Shp1 KO
p-Tyr
Src p-Tyr418
tubulin
Syk p-Tyr519/20
Syk
SFK p-Tyr418 normalised to tubulin
Syk p-Tyr519/20 normalised to Syk

Figure 7

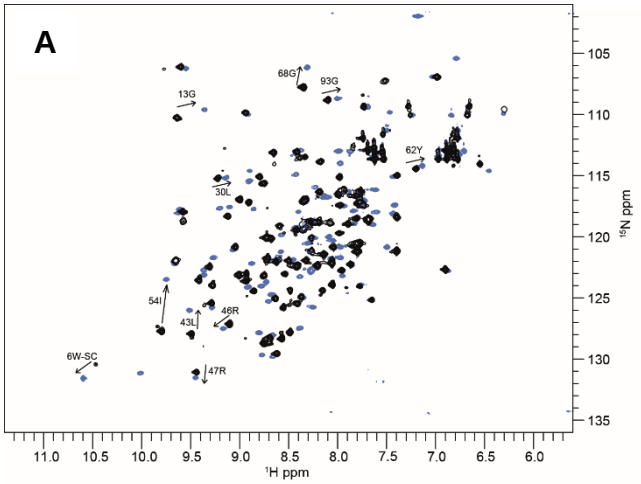
A
68G
93G
13G
62Y
30L
54I
43L
46R
6W-SC
47R
105
110
115
120
125
130
135
11.0
10.5
10.0
9.5
9.0
8.5
8.0
7.5
7.0
6.5
6.0
¹H ppm
¹⁵N ppm

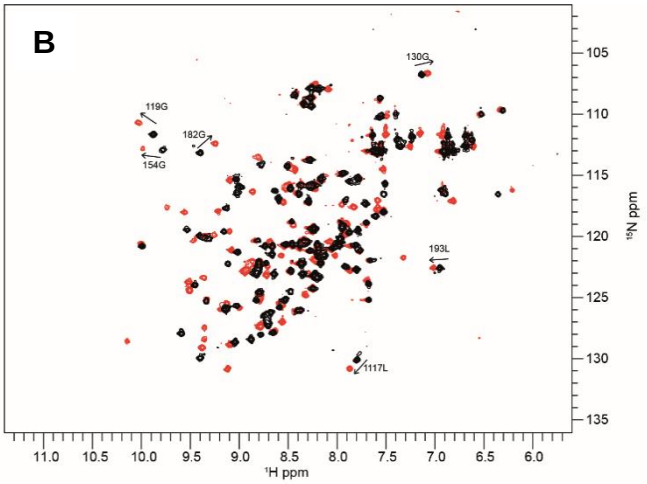
B
130G
119G
182G
154G
193L
117L
105
110
115
120
125
130
135
11.0
10.5
10.0
9.5
9.0
8.5
8.0
7.5
7.0
6.5
6.0
¹H ppm
¹⁵N ppm

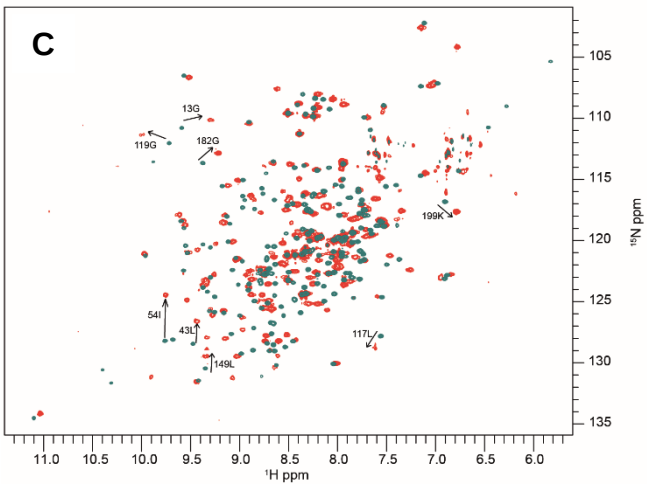
C
13G
119G
182G
199K
54I
43L
149L
117L
105
110
115
120
125
130
135
11.0
10.5
10.0
9.5
9.0
8.5
8.0
7.5
7.0
6.5
6.0
¹H ppm
¹⁵N ppm

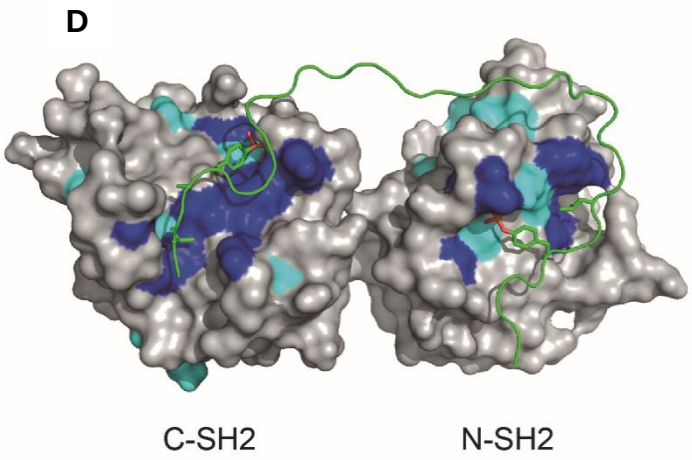
D
C-SH2
N-SH2

Supplementary Methods

Generation of G6b-B diY/F mice

A constitutive *knock-in* (*KI*) strategy was used to generate *G6b-B diY/F KI* mice (Figure S1). A targeting vector containing the mutated *G6b* gene and a *puromycin resistance cassette* (*PuroR*) flanked with flippase recognition target (FRT) sites was produced. Point mutations were inserted into the *G6b* gene, converting the tyrosine codons TAC and TAT of exon 6 (positions 648 and 726 within the transcript nucleotide sequence, taken from NM_001191012.1) to TTC, the codon for phenylalanine. Neighboring genes were also cloned into the targeting vector, providing 7 kb and 4 kb homology arms. These allow for insertion of the mutant gene, via homologous recombination, into germline competent C57Bl6/NTac embryonic stem cells. This effectively knocks out the *WT G6b* gene and replaces it with the mutant gene, called *G6b-B diY/F*. Recombined mutants with the correctly inserted mutant construct were isolated using the *PuroR* gene positive- and thymadine kinase negative-selection. Following validation, clones were injected into mouse blastocysts and transferred into pseudopregnant female mice. *G6b-B diY/F* mice were subsequently crossed with Tg(CAG-flpe) Flp recombinase expressing mice, causing excision of the FRT sites, therefore removing the *PuroR* cassette and generating the final *G6b-B diY/F* constitutive *KI* mouse allele. Further crossing with C57Bl6/NTac mice and selective breeding removed expression of Flp recombinase in animals used for experiments.

Successful targeted *KI* was shown by PCR using oligos 1 & 2 and 5 & 6.

The residual FRT site following excision of the *PuroR* gene allows for the *WT* and *KI* alleles to be distinguished by PCR. Primers were generated to target the annealing sites indicated by oligos 3 and 4 (Figure 3.1Aiv). These produce a PCR product of

315 base pairs (bp) for the *WT* allele and 401 bp for the KI allele, which can be distinguished by running the PCR.

Mouse G6b-specific antibodies

The anti-mouse monoclonal antibody was raised by injection of Fc-fused G6b-B ectodomain into rats. As such, this antibody will recognize both G6b-A-like and G6b-B isoforms on the surface of platelets. Anti-mouse G6b-B polyclonal antibody was generated by injection of a peptide specific to G6b-B into rabbits. These were generated as previously described.[1]

Platelet clearance

Mice were injected intravenously with 600 μg of N-hydroxysuccinimidobiotin (NHS)-Biotin in PBS. Blood samples were collected from tail veins, into 5 mM EDTA, 10% fetal bovine serum in PBS, at the following time points following injection: 1 hour (h) (Day 1), 24h (Day 2), 48h (Day 3), 72h (Day 4) and 96h (Day 5). Percentage of biotin positive platelets was measured by flow cytometry using PE-Streptavidin (BD Pharmingen, Oxford, UK).

Platelet recovery

Platelets were depleted by intraperitoneal (I.P.) injection of 1.5 μg anti-GPIbα antibody (Emfret Analytics, Wurzburg, Germany) per gram of mouse body weight. Blood samples were collected from the tail vein into 20 mM EDTA in PBS before I.P. injection (Day 0) and at 24 hour intervals following this. Platelet counts were measured using an ABX Pentra 60 hematological counter (Horiba Medical, Northampton, UK).

Platelet clearance and recovery analysis

Proportionate slopes were calculated for each mouse using data from days one to five and days two to seven for platelet clearance and recovery assays, respectively. These slopes were taken as a measurement of rate of platelet clearance (% of platelets per day) and rate of platelet production ($\times 10^8$/mL platelets per day).

Immunohistochemistry

Spleens and femurs from *G6b-B diY/F* and *WT* mice were fixed in buffered formalin and embedded in paraffin. Sections were H&E and reticulin stained and examined by light microscopy with a Zeiss Axio ScanZ1 (Carl Zeiss Ltd, Cambridge, UK).

Tail bleeding assay

Mice were anaesthetized using isoflurane and placed on a raised heating pad at 37°C. 5 mm of the tail tip was excised using a scalpel blade and blood drops collected (falling in air) to a maximum time of 20 minutes, or 5 minutes with no blood drop falling. Bleeding tendency was quantified by determining the mass of blood loss (mg) following injury and dividing by the weight of the mouse (g). A maximum allowed blood loss was calculated for each mouse equal to ≤10% of body weight. Blood loss for all animals remained within this limit. Where the blood loss was recorded as zero (n=1) a value equal to the average of zero and 50% of the limit of detection (0.1 mg blood loss) was employed.

Blood loss (mg/g) was modelled as a bi-modal function, comprising of a gamma distribution representing a low (normal) bleeding tendency and a normal distribution representing increased bleeding. The probability that a mouse of a specified genotype had a normal bleeding time was P_{norm} or was a bleeder was $(1 - P_{norm})$. Probabilities were modelled as logits. ($\text{logit}(P) = \ln(P/(1-P))$)

The maximum likelihood (-2LL = -2 × log likelihood) was determined generating parameters that defined normal and increased bleeding and the logits of the probabilities of each genotype having normal bleeding. Likelihood ratio tests were performed to determine whether the probability of bleeding differed between genotypes.

Modelling was done in Microsoft Excel (Redmond, WA, USA) and replicated in NONMEM 7.3 (Icon PLC, Dublin, Ireland) to generate standard error values for the parameters.

Flow cytometry

Mice were CO_2-asphyxiated and blood collected from the vena cava into 1/10 (v/v) acid-citrate-dextrose anticoagulant. Fluorescein isothiocyanate (FITC)-conjugated antibodies were used to measure surface receptor expression in whole blood with an Accuri C6 flow cytometer (BD Biosciences, Oxford, UK). Values for relevant IgG controls have been subtracted from all presented data. For flow cytometry based activation assays, whole blood or 2×10^7/mL washed platelets were stained with FITC-conjugated P-selectin antibody or Alexa488-conjugated fibrinogen in the absence (basal) and presence of indicated agonists. Thrombin stimulations were performed in the presence of 10 μM GPRP to prevent fibrin polymerization. For all flow cytometry 10,000 events were collected and data is presented as median fluorescence intensity. Reactions were terminated with cold 1% paraformaldehyde in PBS. The proportion of reticulated platelets in whole blood was quantified by flow cytometry following 30 minute incubation with BD Retic-Count solution (BD Biosciences, Oxford, UK).

Platelet adhesion and spreading on fibrinogen

Washed platelets (2 × 10^7/mL) were prepared as previously described in modified Tyrodes buffer (134 mM NaCl, 2.9 mM KCl, 340 μM Na_2HPO_4•$12H_2O$, 12 mM $NaHCO_3$, 20 mM HEPES, 1 mM $MgCl_2$, 5 mM glucose, pH 7.3, 37°C).[2] Platelet spreading assay on fibrinogen-coated coverslips was performed as previously described.[3] All slides were imaged using a Zeiss Axiovert 200M microscope and quantified using ImageJ. Stages of platelet spreading were categorized as unspread, formation of filopodia, formation of lamellipodia and fully spread (Figure S6).

Platelet aggregation and secretion

Platelet aggregation and adenosine triphosphate (ATP) secretion was measured in washed platelets (2 × 10^8/mL) using a Chrono-Log Model 700 lumi-aggregometer (Havertown, PA, USA), as previously described.[4] ADP-sensitive platelets were prepared as previously described,[5] using modified Tyrodes buffer supplemented with 0.02 U/mL apyrase for washing steps. The final platelet pellet was resuspended in modified Tyrodes buffer without apyrase and before starting aggregations 1 μM $CaCl_2$ and 50 μg/mL fibrinogen was added to the diluted platelets. Aggregation traces were exported and mean traces calculated.

Platelet flow adhesion coverslip preparation

Glass coverslips (24 × 60 mm) were coated with three microspots (0.5 μL/spot), which produce thrombi via different platelet-adhesive receptors (De Witt, Nat Comm 2014). The microspot coatings contained (in the direction of flow): (i) von Willebrand factor-binding peptide (VWF-BP, 12.5 mg/mL, purified as described in Lisman, Blood 2006) + laminin (50 μg/mL, from human plasma); (ii) VWF-BP + laminin + rhodocytin

(250 μg/mL, from BioSource and purified as described in Hooley, Biochemistry 2008); (iii) collagen type I (100 μg/mL, Nycomed Pharma, Munich, Germany). The coated coverslips were blocked with modified Tyrode's Hepes buffer pH 7.45 (TH-buffer: 5 mM Hepes, 136 mM NaCl, 2.7 mM KCl, 2 mM $MgCl_2$, 0.42 mM NaH_2PO_4) containing 1% bovine serum albumin and mounted into parallel plate flow chambers.

Platelet flow adhesion

Blood was collected as above into 40 μM PPACK, 5 units (U)/mL heparin and 50 U/mL fragmin (final concentrations) and perfused for 3.5 minutes, at a wall-shear rate of 1000 s^{-1}, over glass coverslips coated with microspots of indicated platelet agonists.[6] Images were captured with an EVOS microscope (Life Technologies, Carlsbad, CA, USA) and analyzed using Fiji (Figure S7).[7]

Platelet flow adhesion image capture and analysis

Immediately after perfusion of blood was complete, brightfield images were captured from each microspot. Thrombi were then stained using TH-buffer containing 1 mg/mL glucose and 1 mg/mL bovine serum albumin, supplemented with 2 mM $CaCl_2$, 1 U/mL heparin, Alexa647-conjugated annexin A5 (1:200, Invitrogen Life Technologies, Carlsbad, CA, USA), FITC-conjugated anti-P-selectin antibody (1:40) and PE-conjugated anti-JON/A antibody (1:20). Per microspot, 2 (brightfield) or 3 (fluorescence) representative images were taken and analyzed.

Recorded images were analyzed using semi-automated scripts written in Fiji software (Laboratory for Optical and Computational Instrumentation at the University of Wisconsin-Madison, USA). This resulted in percentages of surface area coverage (%SAC) of deposited platelets/thrombus (from brightfield images), and of %SAC of platelet/thrombus fluorescence per fluorescent label. In addition, brightfield images

were analyzed for a morphological score (scale 0-5), thrombus contraction score (scale 0-3) and thrombus height (multilayer, scale 0-3) in comparison to reference images, to provide an indication of the overall size and height of platelet aggregates on the microspots (Figure S7, De Witt, Nat Comm 2014). Finally, the %SAC of multilayered thrombi was analyzed by manual coloring in Fiji.

Platelet biochemistry

All stimulations were conducted in the presence of 10 μM lotrafiban, 37°C with constant stirring at 1,200 rpm. Whole cell lysates were prepared, immunoprecipitations performed and resolved by SDS-PAGE, as previously described,[8] using washed platelets at 4-5 × 10^8/mL. Band intensities were quantified using ImageJ and normalized to reblots of either pan-Syk or tubulin as stated in Figure Legends.

Protein production for structural analysis of G6b-B-Shp2 interaction

Human G6b-B p-ITIM (residues 206-215; EPSLL[pY]ADLD), p-ITSM (residues 232-241; DASTI[pY]AVVV) and dual p-ITIM/p-ITSM (residues 206-241; EPSLL [pY]ADLDHLALSRPRRLSTADPADASTI[pY]AVVV) peptides were synthesized by Alta Bioscience (Birmingham, UK) or Genscript (NJ, USA). All peptides were N-terminally acetylated, while only p-ITIM was C-terminally amidated. The individual human SH2 domain constructs were provided by Tony Pawson (University of Toronto). The tandem SH2 domain construct containing residues 4-216 of wild-type Shp2, preceded by a TEV protease cleavable poly-histidine tag, was inserted into a pNIC28-Bsa4 vector obtained from SGC (Oxford, UK) by ligation independent cloning. Proteins were expressed in E. coli using minimal M9 media with $^{15}NH_4Cl$ as the sole nitrogen source and, for assignment purposes, uniformly labeled ^{13}C-

glucose as the sole carbon source. Proteins were purified using Ni-NTA affinity columns followed by size exclusion chromatography.

Structural analysis of G6b-B-Shp2 interaction

NMR spectroscopy was performed at 25°C using a 600 MHz Varian Direct Drive spectrometer for the individual SH2 domains and an 800 MHz Varian Inova spectrometer for the tandem SH2 constructs. Protein concentrations for all titrations were 400 µM. Spectra were processed using NMRpipe,[9] and analyzed using CCPN analysis.[10] Model structures of tandem SH2 binding to the phosphorylated C-terminal tail of G6b-B were generated using HADDOCK.[11,12]

For residue-specific NMR assignments either BEST (Lescop et al. 2007) (for the individual SH2 domains) or standard versions (for the tandem SH2) of HNCOCA, HNCA, HNCO, HNCACO, HNCACB and HNCOCACB spectra were obtained. Titration data were collected using SOFAST-HMQC experiments (Schanda et al. 2005).

For model structures the pdb file 5DF6 (Liu at al. 2016) was used as the template for the protein structure. Binding of the peptide to the protein was assumed to be canonical with respect to the pY pocket. Distance restraints of 7Å between R128-CZ: pY237-P and R32-CZ:pY211-P were used to orientate the peptide with nSH2 binding to ITIM and cSH2 binding to ITSM. Peptide residues outside the canonical SH2 domain recognition site (pY, +1, +3) were allowed to be fully flexible during the HADDOCK calculation as were the residues linking the two SH2 domains (102-110). Initial peptide complex structure generation and model visualization was performed using PyMOL (Schrödinger, Cambridge, UK).

References

1. Mazharian A, Wang YJ, Mori J, et al. Mice lacking the ITIM-containing receptor G6b-B exhibit macrothrombocytopenia and aberrant platelet function. *Sci Signal*. 2012;5(248):ra78.
2. Senis YA, Atkinson BT, Pearce AC, et al. Role of the p110delta PI 3-kinase in integrin and ITAM receptor signalling in platelets. *Platelets*. 2005;16(3-4):191-202.
3. McCarty OJ, Larson MK, Auger JM, et al. Rac1 is essential for platelet lamellipodia formation and aggregate stability under flow. *J Biol Chem*. 2005;280(47):39474-39484.
4. Senis YA, Tomlinson MG, Ellison S, et al. The tyrosine phosphatase CD148 is an essential positive regulator of platelet activation and thrombosis. *Blood*. 2009;113(20):4942-4954.
5. Ohlmann P, Eckly A, Freund M, Cazenave JP, Offermanns S, Gachet C. ADP induces partial platelet aggregation without shape change and potentiates collagen-induced aggregation in the absence of Galphaq. *Blood*. 2000;96(6):2134-2139.
6. de Witt SM, Swieringa F, Cavill R, et al. Identification of platelet function defects by multi-parameter assessment of thrombus formation. *Nature Communications*. 2014;5.
7. Schindelin J, Arganda-Carreras I, Frise E, et al. Fiji: an open-source platform for biological-image analysis. *Nat Methods*. 2012;9(7):676-682.
8. Pearce AC, Senis YA, Billadeau DD, Turner M, Watson SP, Vigorito E. Vav1 and vav3 have critical but redundant roles in mediating platelet activation by collagen. *J Biol Chem*. 2004;279(52):53955-53962.
9. Delaglio F, Grzesiek S, Vuister GW, Zhu G, Pfeifer J, Bax A. NMRPipe: a multidimensional spectral processing system based on UNIX pipes. *J Biomol NMR*. 1995;6(3):277-293.
10. Vranken WF, Boucher W, Stevens TJ, et al. The CCPN data model for NMR spectroscopy: development of a software pipeline. *Proteins*. 2005;59(4):687-696.
11. van Zundert GC, Rodrigues JP, Trellet M, et al. The HADDOCK2.2 Web Server: User-Friendly Integrative Modeling of Biomolecular Complexes. *J Mol Biol*. 2016;428(4):720-725.
12. Wassenaar TA, de Vries S, Bonvin AM, Bekker H. SQUEEZE-E: The Optimal Solution for Molecular Simulations with Periodic Boundary Conditions. *J Chem Theory Comput*. 2012;8(10):3618-3627.

Table S1. Offspring from het × het breeding pairs

Genotype	Expected frequency	Observed frequency
WT (G6b$^{+/+}$)	25% (60)	29% (70)
Heterozygous (G6b$^{+/diYF}$)	50% (121)	46% (111)
Homozygous (G6b$^{diYF/diYF}$)	25% (60)	25% (60)
Total	100% (241)	100% (241)

Data was collected from 13 breeding pairs (*G6b$^{+/diYF}$* × *G6b$^{+/diYF}$*) and analysed using χ^2 test (P = 0.2875)

Table S2. Peripheral blood cell counts

Haematological parameters	***WT*** (mean ± SD, n=24)	***G6b-B diY/F*** (mean ± SD, n=24)
Platelets (10^9/L)	1093 ± 230	258 ± 64***
Mean platelet volume (fL)	5.8 ± 0.2	7.9 ± 1.8***
Plateletcrit (%)	0.41 ± 0.10	0.10 ±0.06***
Red blood cells (10^{12}/L)	10.9 ± 0.6	10.4 ± 1.1
Hematocrit (%)	31.8 ± 2.6	29.4 ± 3.7*
White blood cells (10^9/L)	8.3 ± 4.6	9.8 ± 4.3
Lymphocytes (10^9/L)	5.5 ± 3.4	12.5 ± 4.6***
Monocytes (10^9/L)	0.70 ± 0.60	0.90 ± 0.60
Neutrophils (10^9/L)	0.65 ± 0.45	1.10 ± 0.76*
Eosinophils (10^9/L)	0.01 ± 0.04	0.00 ± 0.04
Basophils (10^9/L)	0.39 ± 1.39	0.10 ± 0.27

* indicates P<0.05 and *** indicates P<0.001 with Students t-test

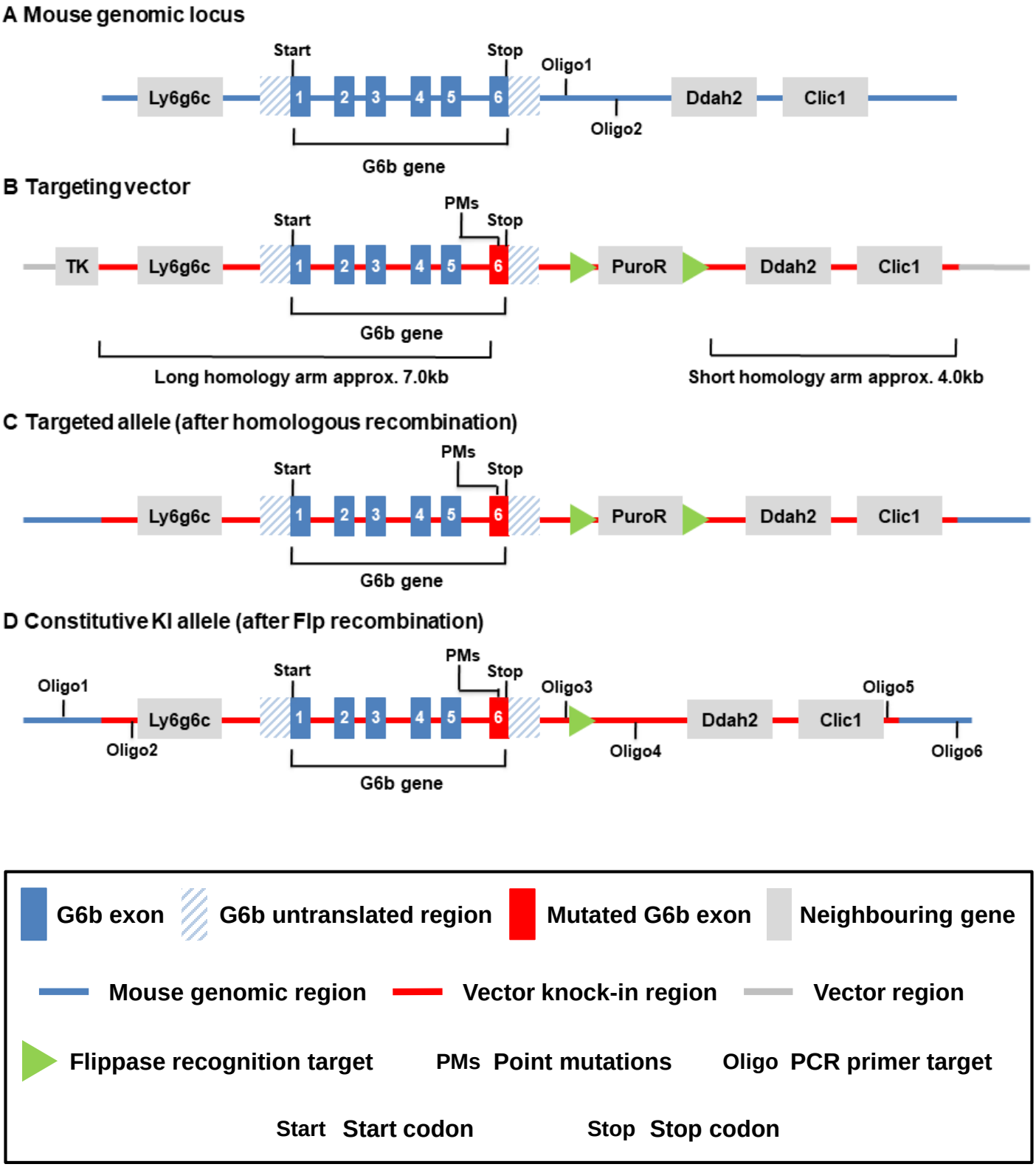

Figure S1. Targeting strategy for constitutive knock-in of *G6b-B diY/F* allele. A constitutive knock-in strategy was used by Taconic to insert a mutated *G6b* allele into (A) the genomic locus of mouse *G6b*. (B) A targeting vector containing point mutations within exon 6 and a puromycin resistance cassette flanked by Flp recombinase sites was produced. (C) The two homology arms of the targeting vector flanking the mutated exon 6 provided sites for homologous recombination to insert the mutated gene into the C57BL/6NTac embryonic stem cell genome. (D) The puromycin resistance was removed by crossing mice expressing the G6b-B diY/F allele with a Flpe recombinase expressing mouse producing the final constitutive knock-in allele.

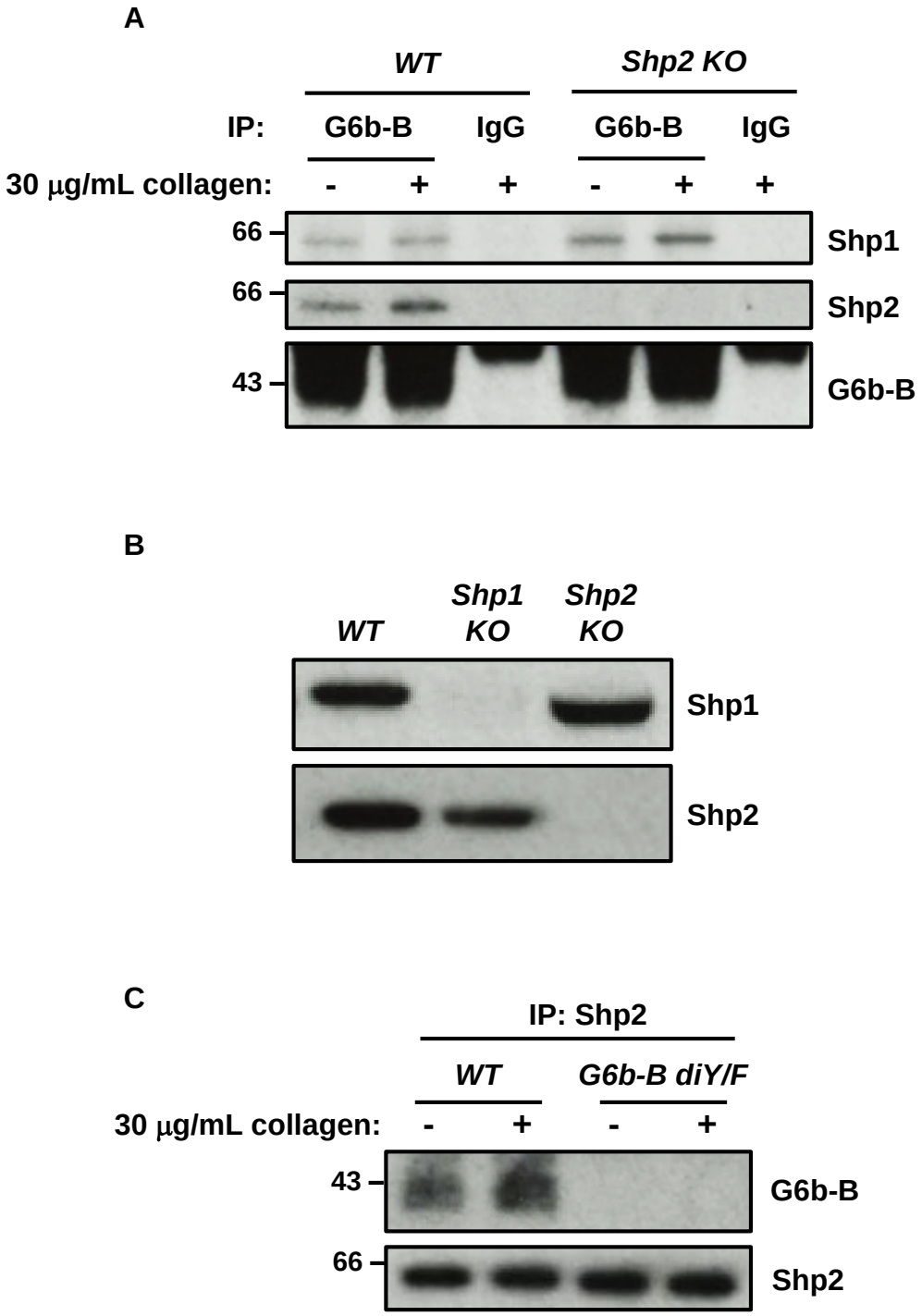

Figure S2. Interaction of G6b-B with Shp1 and Shp2. (A) Immunoprecipitation of G6b-B in *WT* and *Shp2 KO* mouse washed platelets (4×10^8/mL) was performed to investigate the specificity of Shp1 and Shp2 antibodies. (B) Specificity of Shp1 and Shp2 antibodies were also investigated in whole cell lysates from *WT*, *Shp1 KO* and *Shp2 KO* mouse platelets. (C) Basal and 30 μg/mL collagen activated platelets were lysed and Shp2 immunoprecipitated to investigate the co-immunoprecipitation of G6b-B. Representative blots from two independent experiments.

A

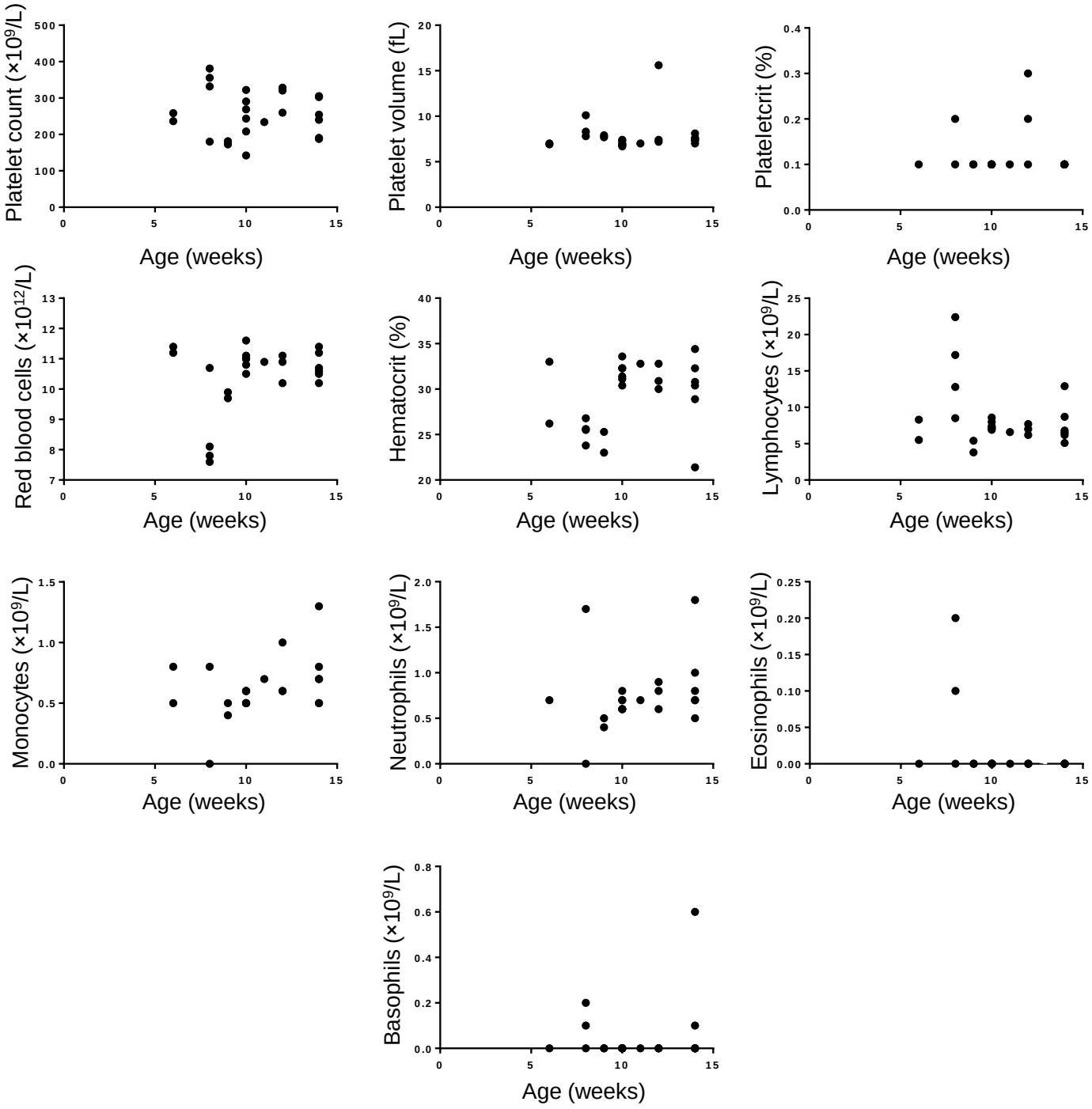

B

	Platelet count	Platelet volume	Plateletcrit	Red blood cells	Hematocrit	Lymphocytes	Monocytes	Neutrophils	Eosinophils	Basophils
R^2	0.00	0.00	0.01	0.09	0.08	0.07	0.21	0.12	0.13	0.02
P-value	0.80	0.13	0.63	0.15	0.18	0.22	0.02	0.10	0.09	0.49

Figure S3. Blood cell counts variation is independent of age in *G6b-B diY/F* mice. (A) Blood cell counts were plotted against age for *G6b-B diY/F* mice (n=24). (B) Regression analysis indicates that there is no correlation between age and hematological parameters.

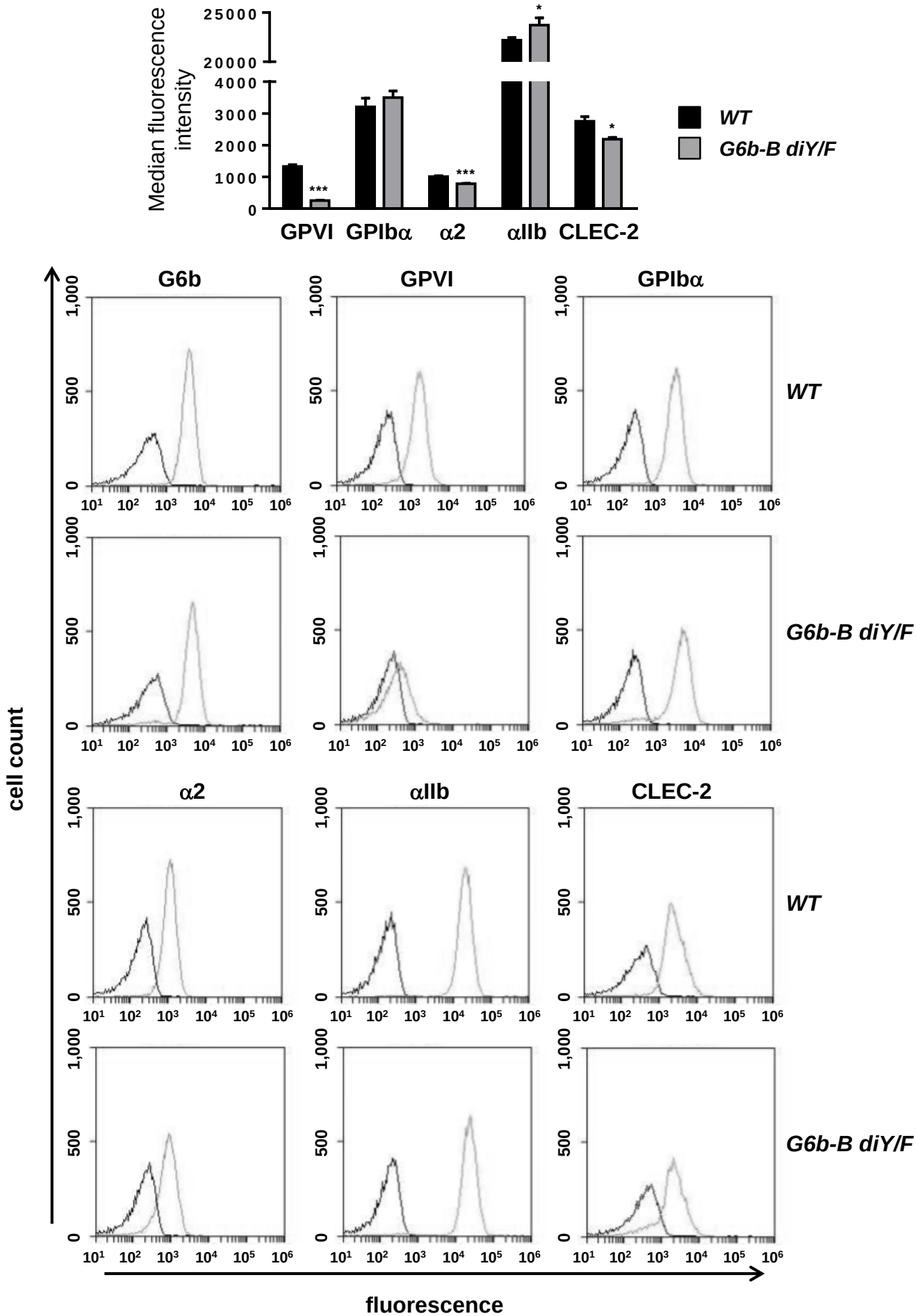

Figure S4. Quantification of surface receptor expression. (A) Median fluorescence intensity (mean ± SEM, n=5-6, * $P<0.05$, *** $P<0.001$). (B) Representative histograms. IgG control (dark grey) and respective staining (light grey).

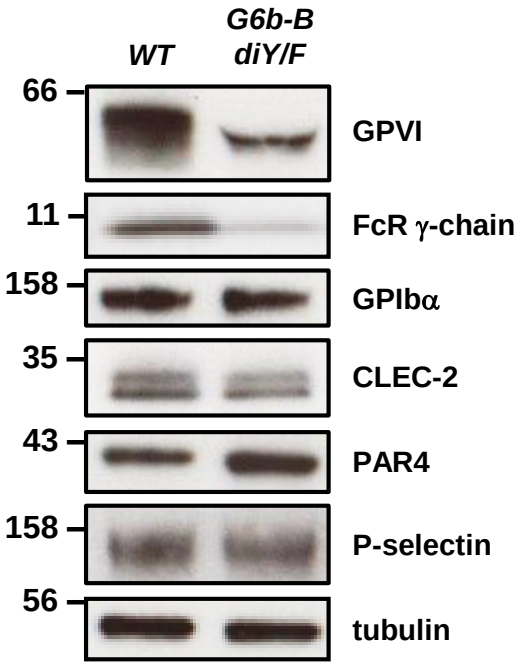

Figure S5. Total protein expression levels. Lysates were prepared from washed platelets (4×10^8/mL).

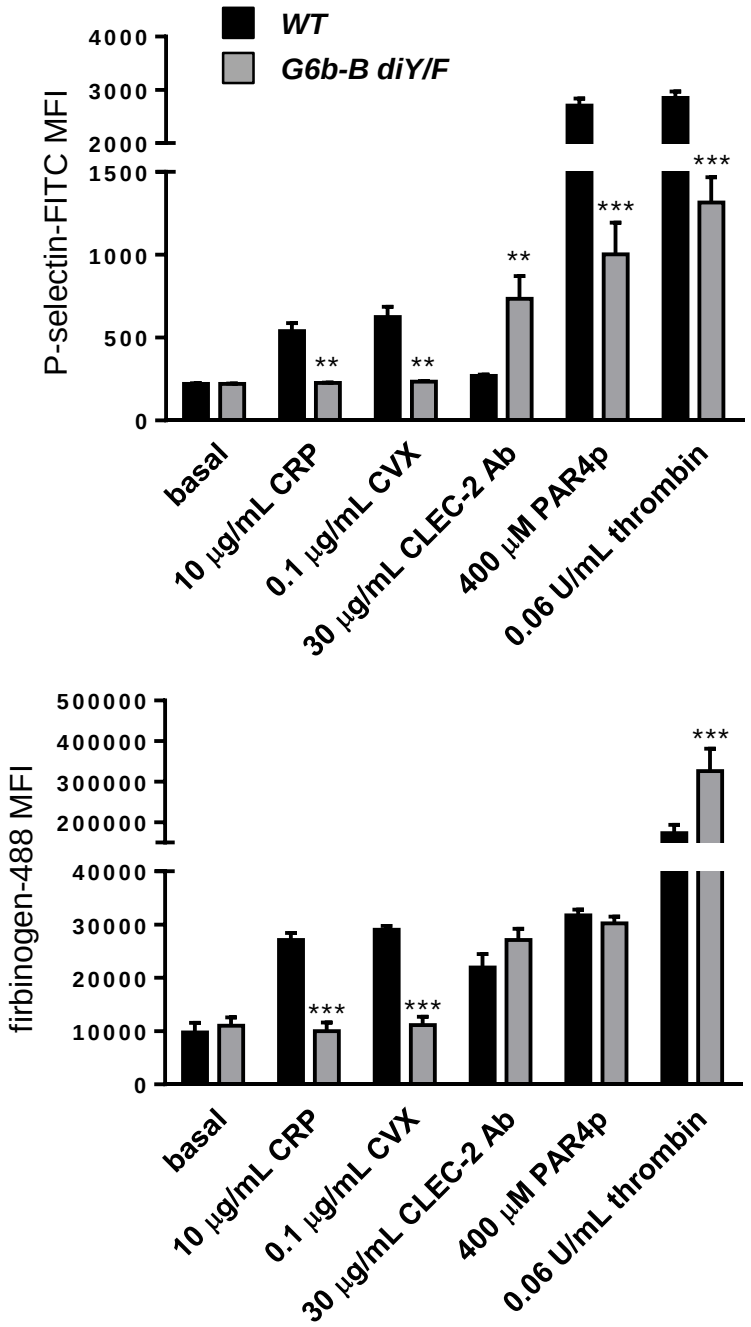

Figure S6. P-selectin exposure and fibrinogen binding in washed platelets. (A) anti-P-selectin-FITC and (B) fibrinogen-488 binding to washed platelets (2×10^7/mL) following stimulation with the indicated agonists. Mean ± SEM, n=5, ** P<0.01, *** P<0.0001.

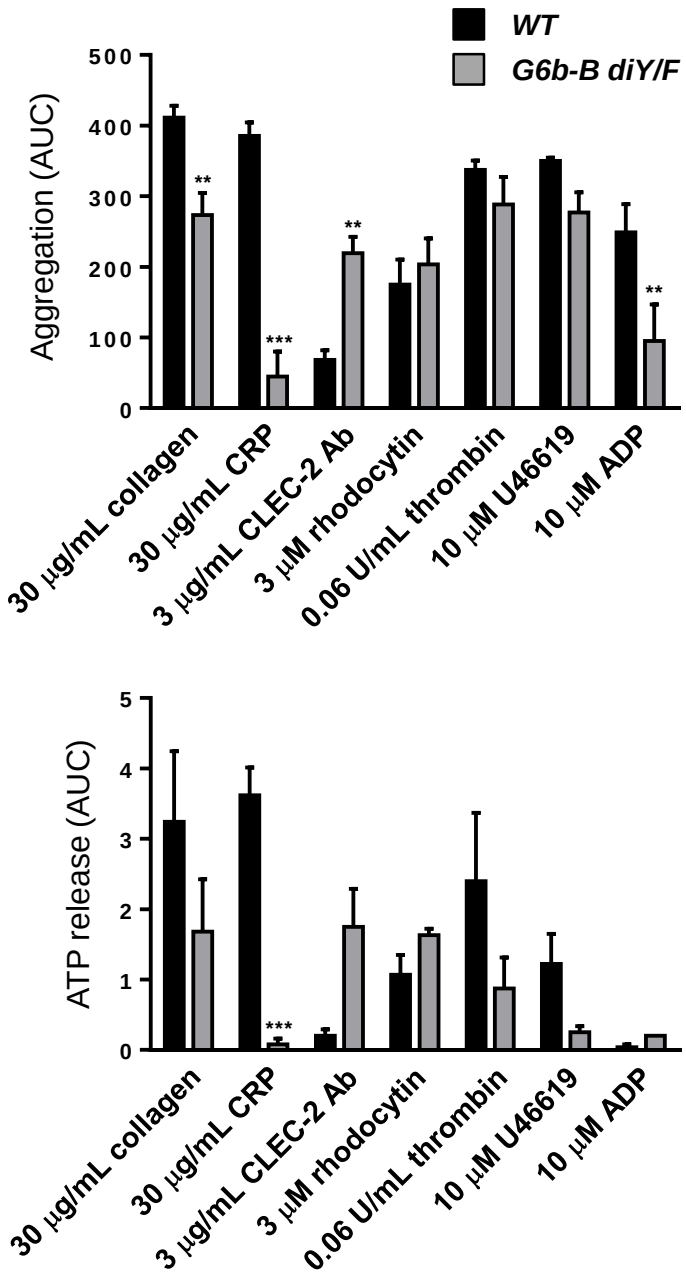

Figure S7. Analysis of aggregation and ATP release. Washed platelets (2×10^8/mL) were activated with the indicated agonists in a lumi-aggregometer. For ADP stimulations platelets were washed in the presence of 0.02 U/mL apyrase and once prepared supplemented with 1 μM $CaCl_2$ and 50 μg/ml fibrinogen. Area under the curve (AUC) of aggregation and ATP release was analysed, mean ± SEM, n=3-5, ** P<0.01, *** P<0.0001.

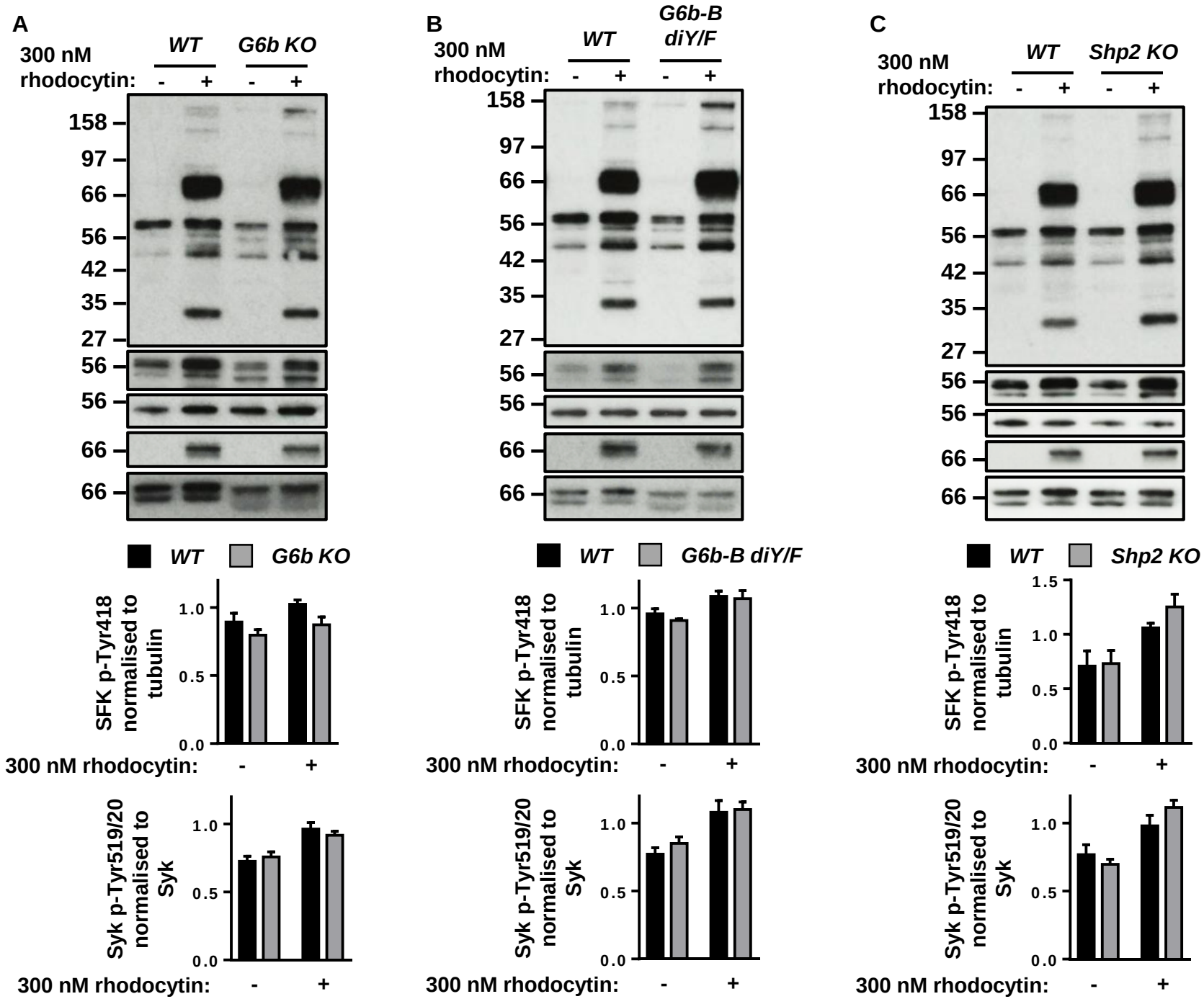
A
300 nM rhodocytin:
WT
G6b KO
158
97
66
56
42
35
27
56
56
66
66
WT
G6b KO
SFK p-Tyr418 normalised to tubulin
1.0
0.5
0.0
300 nM rhodocytin: - +
Syk p-Tyr519/20 normalised to Syk
1.0
0.5
0.0
300 nM rhodocytin: - +
B
300 nM rhodocytin:
WT
G6b-B diY/F
158
97
66
56
42
35
27
56
56
66
66
WT
G6b-B diY/F
SFK p-Tyr418 normalised to tubulin
1.0
0.5
0.0
300 nM rhodocytin: - +
Syk p-Tyr519/20 normalised to Syk
1.0
0.5
0.0
300 nM rhodocytin: - +
C
300 nM rhodocytin:
WT
Shp2 KO
158
97
66
56
42
35
27
56
56
66
66
WT
Shp2 KO
SFK p-Tyr418 normalised to tubulin
1.5
1.0
0.5
0.0
300 nM rhodocytin: - +
Syk p-Tyr519/20 normalised to Syk
1.0
0.5
0.0
300 nM rhodocytin: - +

Figure S8. Rhodocytin signalling in *G6b-B diY/F*, *G6b KO* and *Shp2 KO* mouse platelets. Washed platelets (4 × 10^8/mL) from indicated genotypes were activated with 300 nM rhodocyin, 3 minutes, 10 μM lotrafiban, 37ºC, 1200 rpm stirring. Stimulations were terminated by lysing cells and proteins were resolved by SDS-PAGE to investigate signalling events using the inidicated phospho-specific antibodies. Src p-Tyr418 and Syk p-Tyr519/20 were quantified using ImageJ. Representative blots from n=3-4.

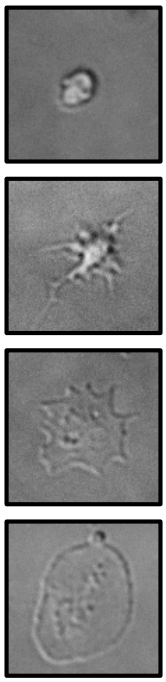

Figure S9. Platelet spreading on fibrinogen scoring categories

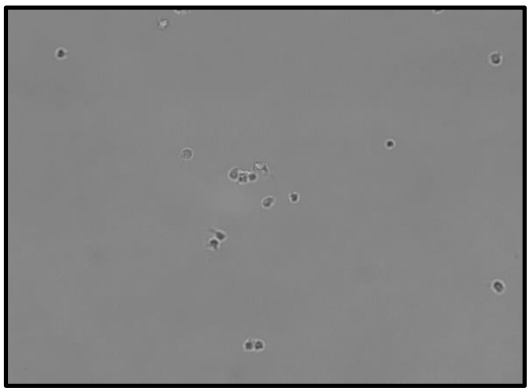

Morphological score: 0
Contraction score: 0
Multilayer score: 0

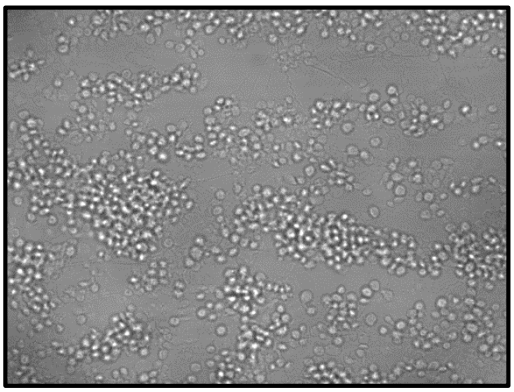

Morphological score: 3
Contraction score: 1
Multilayer score: 1

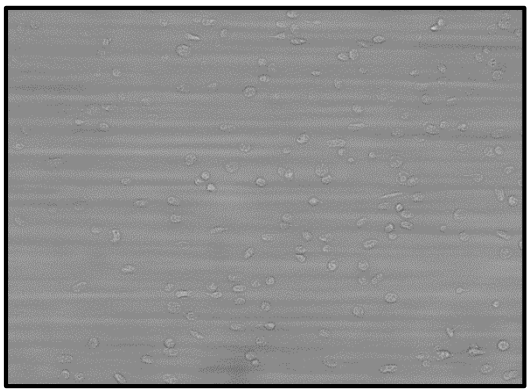

Morphological score: 1
Contraction score: 0
Multilayer score: 0

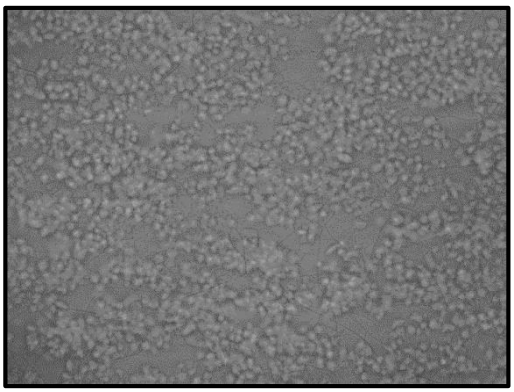

Morphological score: 4
Contraction score: 2
Multilayer score: 2

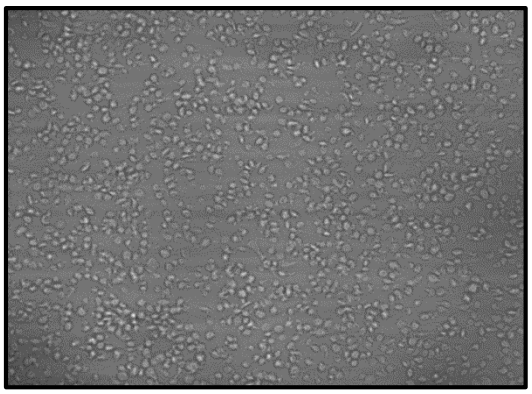

Morphological score: 2
Contraction score: 0
Multilayer score: 0

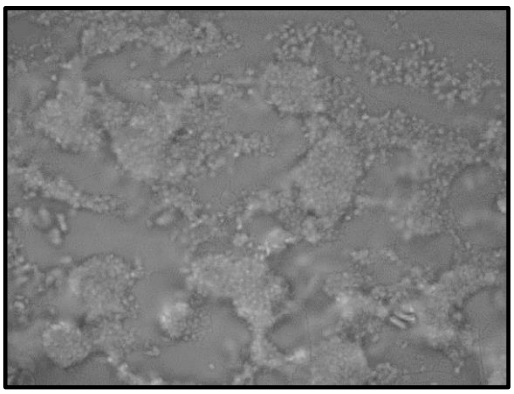

Morphological score: 5
Contraction score: 3
Multilayer score: 3

Figure S10. Platelet flow adhesion morphological scoring representative images